IEEE Access
Multidisciplinary | Rapid Review | Open Access Journal

Received March 27, 2022, accepted April 14, 2022, date of publication April 25, 2022, date of current version May 20, 2022.

Digital Object Identifier 10.1109/ACCESS.2022.3170106

Metasurface-Aided Wireless Power Transfer and Energy Harvesting for Future Wireless Networks

HENRY OJUKWU[1], BOON-CHONG SEET[1], (Senior Member, IEEE), AND SAEED UR REHMAN[2], (Senior Member, IEEE)

[1]Department of Electrical and Electronic Engineering, Auckland University of Technology, Auckland 1010, New Zealand
[2]College of Science and Engineering, Flinders University, Bedford Park, Adelaide, SA 5042, Australia

Corresponding author: Boon-Chong Seet (boon-chong.seet@aut.ac.nz)

ABSTRACT The desire for battery longevity and ubiquitous wireless charging of mobile devices is driving researchers to explore divergent strategies to extract and harness energy from ambient radio frequency (RF) signals. Different rectenna designs to convert or rectify energy from electromagnetic (EM) signals into direct current (DC) have been explored for wireless power transfer (WPT) and wireless energy harvesting (WEH). However, these rectennas are characterized by low energy capturing and RF-to-DC conversion deficiencies, complex rectifier design, and bulky size. Recently, man-made materials such as metasurfaces with unique EM properties have emerged to address these limitations of existing rectenna systems. This paper presents a comprehensive survey of not only the state-of-the-art advances in metasurface-aided WPT and WEH systems, but also their applications to emerging technologies for future wireless networks such as wireless powered communication network (WPCN), simultaneous wireless information and power transfer (SWIPT), and millimeter wave (mmWave) communication. Besides discussing the research challenges and opportunities, we also present our proposed approach of harnessing metasurface technology to enhance end-to-end energy delivery in future wireless networks.

INDEX TERMS Metasurface, wireless power transfer, wireless energy harvesting, wireless powered communication network, simultaneous wireless information and power transfer, millimeter wave communication, end-to-end energy delivery, reconfigurable intelligent surface.

I. INTRODUCTION

The next generation of wireless communication systems, dubbed as the sixth generation (6G) system, is expected to fulfil the increasing demand for low energy usage and high efficiency energy delivery for ubiquitous wireless charging of mobile devices using radio frequency (RF) energy sources [1]. Future connected devices will be able to harvest energy from surrounding RF signals anytime, anywhere, to recharge themselves in order to remain indefinitely operational without having to seek a mains power outlet for plug-in charging [2]. This capability is not only important for users of mobile communication devices, but also for sensors employed in particular for outdoor environmental or structural monitoring [3]. One promising alternative to conventional rectennas that could uplift the RF energy harvesting and power transfer performance for 6G systems is the two-dimensional artificially engineered materials known as metasurfaces [4].

Metasurfaces exhibit the ability to spatially process energy signals without requiring amplifiers or active phase shifters. Hence, with metasurfaces, the RF power can be efficiently transferred from one point to another at minimal costs. The metasurface concept can be likened to the technology of massive multiple-input multiple-output (MIMO), where large arrays of antenna elements are utilized to improve the spectral and energy efficiencies of wireless networks [5]. However, unlike massive MIMO that can only optimize the communication end points, metasurfaces are programmable that can be tuned to achieve favorable propagation conditions for the RF signals [6], [7], either for information or energy delivery. Furthermore, metasurfaces have simpler structure and higher beamforming gain that can be exploited for wireless power transfer (WPT) and wireless energy harvesting (WEH) applications.

Much of this survey is motivated by the growing importance of metasurface technology in mitigating three key

The associate editor coordinating the review of this manuscript and approving it for publication was Ding Xu.

challenges in the practical realization of WPT and WEH systems. Firstly, is the issue of low harvested power levels at the energy receivers due to path loss and other propagation factors, resulting in a received amount of energy that is barely sufficient to satisfy the requirement of industrial-grade wireless charging systems. With the capability of a programmable metasurface to create a favorable propagation environment, the issue of low harvested power level due to hostile propagation conditions can be mitigated. Secondly, is the issue of limited power transfer efficiency and energy reception capacity of conventional antennas due to the nature of their structural configurations and materials used, resulting in various types of power losses, including impedance and polarization mismatch power losses (caused by mismatches between transmit and receive antennas in terms of their impedance and polarization); and antenna feed power loss (arising from connectors, couplers, and cables connecting the antenna to its transmitter or receiver circuit). These power losses can be mitigated by using metasurfaces, which are characterized by high impedances for coupling reduction between the antennas; and polarization insensitivity. Thirdly, is the issue of the RF to direct current (DC) conversion efficiency deteriorating with decreasing input power to the rectifier circuit. This explains why rectenna arrays have been commonly used for mitigating this issue. However, rectenna arrays based on conventional patch antennas suffer from bulky size and complex rectifier design, resulting in internal power losses and reduced output voltage. Hence, their replacement by more compact and efficient metasurfaces can be an alternative approach to addressing this issue.

Although there exist reviews on metasurfaces for WPT and WEH [8]–[10], this paper goes beyond these reviews to present a comprehensive survey of not only the state-of-the-art advances in metasurface-aided WPT and WEH systems, but also their applications to emerging technologies for future wireless networks such as wireless powered communication network (WPCN), simultaneous wireless and information power transfer (SWIPT), and millimeter wave (mmWave) communication. We discuss how metasurfaces have been used in each of these emerging technologies to improve the WPT and WEH efficiencies and facilitate their practical realization. In addition, we present our proposed approach of harnessing metasurface technology to enhance end-to-end energy delivery in future wireless networks. The rest of the paper is organized as structured in Fig. 1.

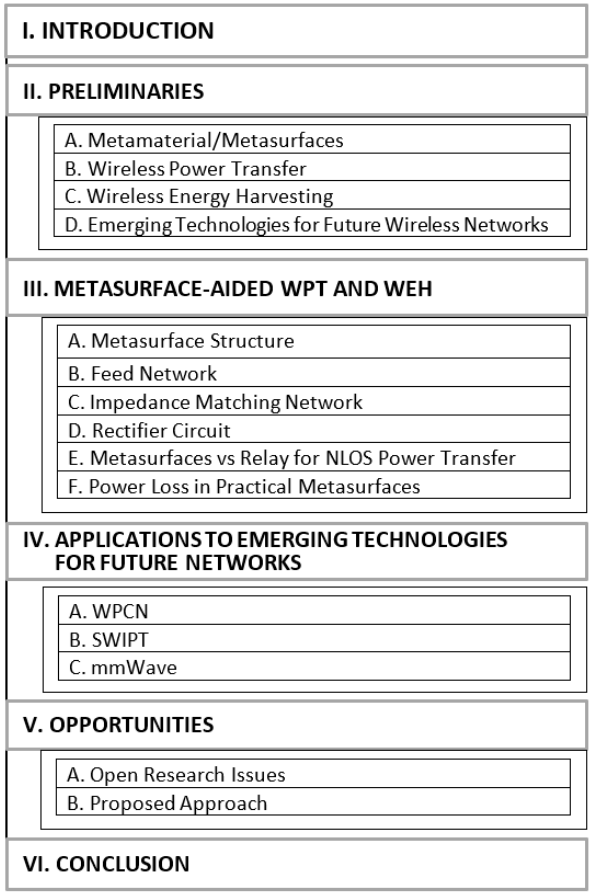

FIGURE 1. Organizational structure of the paper.

II. PRELIMINARIES

This section overviews the basic concepts of metamaterials/metasurfaces, WPT, WEH, and the emerging technologies of WPCN, SWIPT, and mmWave for future wireless networks.

A. METAMATERIALS/METASURFACES

Metamaterials are three-dimensional (3D) artificially engineered EM materials comprising periodic assembly of metallic conducting elements such as metallic rings, rods or spherical particles, which collectively act as an active EM medium with negative permittivity and permeability. On the other hand, metasurfaces are two-dimensional (2D) version of metamaterials. Metasurfaces are periodic structures possessing electrically small elementary scattering particles known as unit-cells or meta-cells. These unit cells can be independently or collectively manipulated to perform anomalous transformations on the incident EM signals resulting in enhanced transmission and reception efficiency. Metasurfaces can be utilized in a wide range of applications including WPT (as energy reflectors) and WEH (as energy absorbers) [11].

High RF absorption is one of the unique features of metasurfaces, which can be achieved by manipulating their EM permeability response such that impinging waves are neither reflected nor retransmitted. This gives them an edge over conventional antennas and arrays in terms of the ability to gather RF energy from free space. Hence, metasurfaces are particularly suited for WEH applications.

B. WIRELESS POWER TRANSFER

Nikola Tesla, in the late 19th century, described the freedom of energy transmission from one point to another without a physical connection to a power source as an ''all-surpassing importance to man''. Thus, WPT will offer remarkable

TABLE 1. Overview of near-field and far-field WPT techniques.

Type	Technique	Frequency	Receptor
Near field	Inductive coupling	Hz-MHz	Wire coils
	Resonance inductive coupling	kHz-MHz	Tuned wire coils
	Magneto dynamic coupling	Hz	Rotating magnets
	Capacitive coupling	kHz-MHz	Electrodes
Far field	Radio wave	MHz-GHz	Rectennas
	Light wave	THz	Photocells

freedom of movement and the capability to energize communication devices using stable and continuous RF energy remotely. WPT is concerned with the transfer of power from RF energy transmitters to energy receivers. Techniques of wireless power transfer can be categorized as radiative (far-field) and non-radiative (near-field) [12].

The non-radiative power transmission is where power is transferred over a short distance (typically between 50−500 mm) by near-field coupling between the energy transmitter and receiver. The coupling techniques used include inductive, resonant inductive, magneto dynamic, and capacitive coupling, which differ mainly in terms of their operating frequency and type of energy receptor used. On the other hand, in radiative power transmission, the energy receiver is located in the far-field region of the energy transmitter (typically two or more wavelength distance away), and the energy signal could be a radio wave or light wave. Table 1 concisely overviews the WPT techniques operating in the near-field and far-field.

In this paper, we focus on radiative WPT using RF energy sources. Radiative power transmission can be realized using either a dedicated or hybrid transmitter. Dedicated power transmitters (DPTs) are transmitters that are deployed at the network edges for the sole purpose of being an RF energy source, transmitting only downlink energy-carrying signals to intended user equipment (UEs) or end devices. Note that DPTs neither receive nor transmit information signals. In contrast, hybrid RF transmitters, sometimes also referred to as hybrid access points (HAPs), can simultaneously transmit both information and energy tones in the same carrier signal. Contrary to DPTs, HAPs can receive uplink information signals from UEs or end devices.

C. WIRELESS ENERGY HARVESTING

WEH is concerned with the reception of power from any RF energy source. Conventionally, WEH is performed using a rectenna (rectifying antenna) system that converts received RF energy into direct current (DC) [13]. The rectenna is typically composed of an array of antennas, feed network, impedance matching network, and rectifier circuit. Two conventional configurations for array-based rectennas are: (i) first-combine last-rectify (RF combining): where the RF power received by array elements is first combined and then rectified to DC; and (ii) first-rectify last-combine (DC combining): where the RF power received by each array element

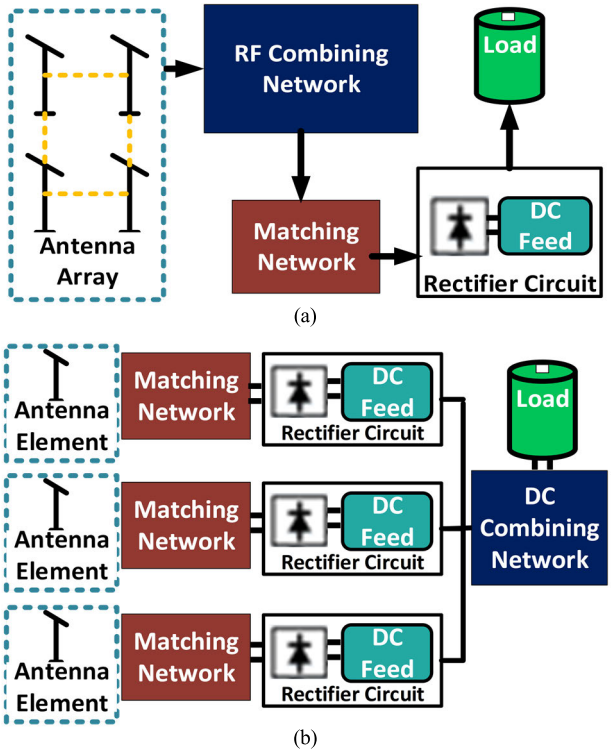

FIGURE 2. Conventional configurations for array-based rectennas: (a) first-combine last-rectify; (b) first-rectify last-combine [14].

is first rectified and the resultant DC from all elements are then combined, as shown in Fig. 2(a), and 2(b), respectively. The RF combining configuration is generally preferred as it leverages the nonlinearity of rectenna more efficiently [14].

The feed network is used for channeling RF power from all array elements into a single outlet for RF or DC combining. Where impedances of the array and rectifier are not identical at the intended operating frequency, an impedance matching network is needed between the array and rectifier for maximum power transfer. Different rectifier circuits exist for RF-to-DC conversion including voltage doubler, floating-gate, and multistage rectifier [15].

D. EMERGING TECHNOLOGIES FOR FUTURE WIRELESS NETWORKS

There are potential applications of WPT and WEH in three emerging technologies for future wireless networks, which are WPCN, SWIPT, and mmWave systems [16].

1) WPCN

This is the concept of a wireless powered communication network where energy-constrained end devices can be wirelessly energized by means of WPT and WEH. The WPT is performed by DPTs or reflecting metasurfaces whereas WEH is performed by end devices, which utilize the energy harvested to transmit or receive information to/from base station (BS) directly, or via the metasurfaces as shown in Fig. 3(a).

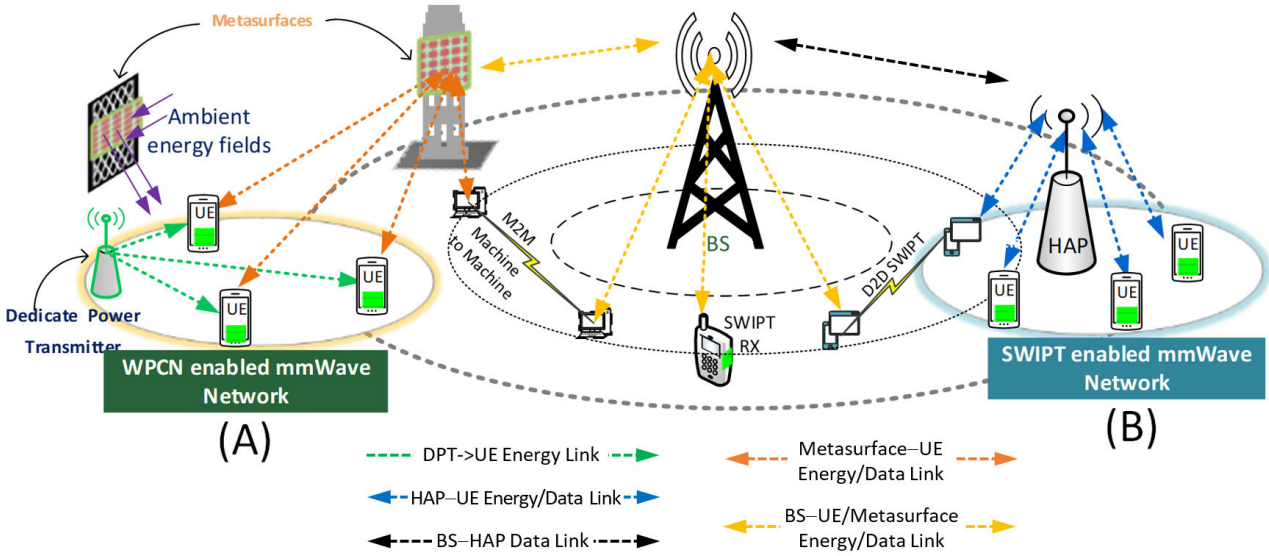

FIGURE 3. Application of WPT and WEH in (a) WPCN; (b) SWIPT.

2) SWIPT

This is the concept of transferring information and power simultaneously over the same RF signal using HAPs, as shown in Fig. 3(b). Thus, the receivers have to decode information and harvest energy from the same RF signal, which can be realized using time switching (TS) or power splitting (PS) technique [17]. In TS, the receiver switches between information decoding and energy harvesting over time. Conversely, PS splits the received RF signal for information decoding and energy harvesting according to a predefined power-splitting ratio.

3) MMWAVE

The mmWave is the frequency range between 30−300 GHz, which has been proposed for future wireless networks due to overcrowding in the microwave spectrum. They can support extremely high data rates due to the vast bandwidth available in mmWave spectrum. However, their high signal frequencies along with atmospheric absorption effects subject their transmissions to high propagation loss. This results in any practical implementation of mmWave network to be characterized by a deployment of ultra-dense small-cell BSs for a given coverage area. Coupled with the use of high-gain massive antenna arrays by BSs, regions covered by mmWave networks can exhibit a high concentration of RF power per unit area [18]. This potentially offers a sustained RF energy source for ubiquitous powering of UEs or end devices at mmWave frequencies.

III. METASURFACE-AIDED WPT AND WEH

The emergence of metasurfaces has offered an attractive alternative to conventional antennas for WPT and WEH due to their greater design flexibility and performance enhancement to RF energy transmission and reception. A complete metasurface-aided WPT and WEH system is composed of four fundamental components: i) metasurface structure; ii) feed network; iii) impedance matching network; and iv) rectifier circuitry. The following sub-sections review advances in each of these constituent components. We then discuss the use of metasurfaces as energy reflectors and their key differences from conventional energy relays. Finally, we discuss the causes of power loss in practical metasurfaces.

A. METASURFACE STRUCTURE

Metasurface structures have been proposed for WPT and WEH applications due to their unique abilities to absorb large amount of EM waves and maintain high energy capturing efficiency at their designed frequencies. Most research on RF energy harvesting have focused on the energy conversion efficiency (ECE), while the energy harvesting efficiency (EHE) of the metasurface structures has received little attention. Recently, the concept of using metasurface resonators as alternative RF energy collectors has been proposed [19], [20], thanks to the unique abilities of metasurfaces to maintain superior EHE at their resonant frequency bands. Unlike conventional patch arrays that have large footprints and wide spacings between adjacent antenna elements, the structural dimension of the metasurface and spacing between the adjacent meta-cells are electrically infinitesimal, which enable more meta-cells to be employed on a given surface area.

The ECE of any energy harvesting system significantly depends on the RF energy collection capacity of its antenna, which can be either a conventional patch array or metasurface structure. The authors in [21] showed that a metasurface structure comprising metallic split ring resonators (SRR) meta-cell arrays can be used to efficiently gather AC equivalent power by attaching the resistive load to the gaps created by the split in individual unit-cell, resulting in high RF to DC

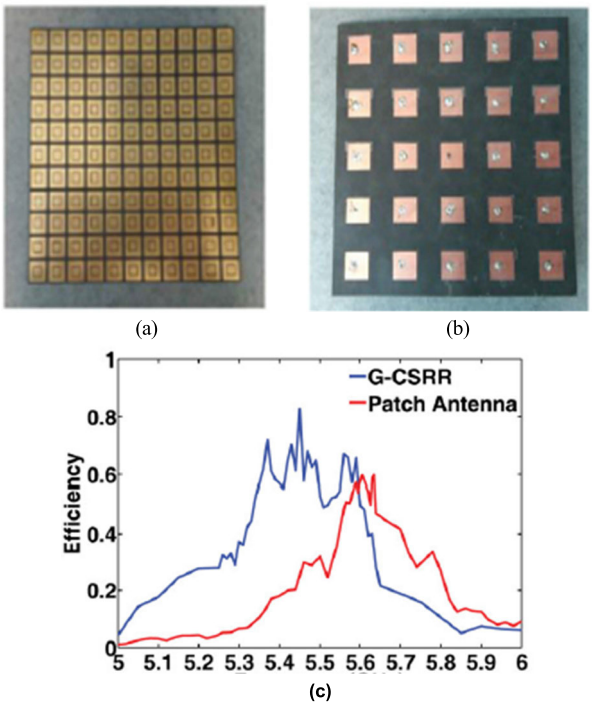

FIGURE 4. (a) Front view of a fabricated 11 × 11 G-CSRR array; (b) Microstrip 5 × 5 patch antenna arrays; and (c) ECE comparison between G-CSRR and microstrip patch arrays [22].

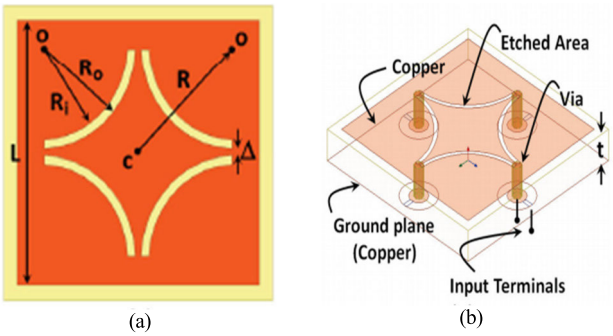

FIGURE 5. (a) Top view of the schematic of a WG-CSRR cell; and (b) Bottom view of four via interconnects forming a 4-port network [23].

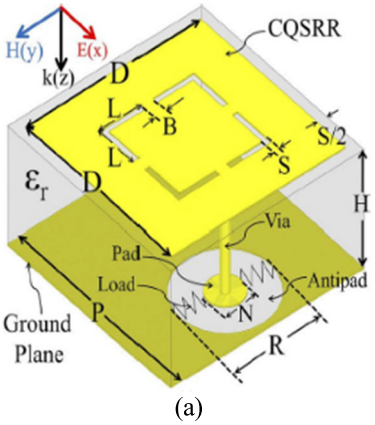

FIGURE 6. 3D geometry of CQSRR metasurface unit-cell [24].

conversion efficiency. The proposed metasurface recorded a conversion efficiency of ∼40% when measured from two rotation angles (30° and 45°), and reached ∼75% when measured from an angle of 60° at 5.8 GHz. A comparative study of the EHE and achievable bandwidth between a ground-backed complementary SRR (G-CSRR) unit-cell array and microstrip patch array was conducted in [22] by measuring the delivered power to the load of each central unit cell and patch antenna element. The EHE was found to be 92%, and 60%, for the metasurface-based G-CSRR array and patch array, respectively. Fig. 4(a) and 4(b) depict the fabricated samples of these two antennas. The superior performance of the G-CSRR can be attributed to the strong resonance and tight coupling between unit cells, which boosts its impedance characteristics and filtering capacity. On the other hand, the patch array performance was adversely affected by the mutual coupling arising from crosstalk between adjacent array elements. Furthermore, the G-CSRR array showed a broader half-power beamwidth (HPBW) than the patch array at a slanting incidence of H- and E- plane excitations. The ECE comparison between the G-CSRR array and microstrip patch antenna array is shown in Fig. 4(c).

In [23], a bow-tie cavity constituting four conductive cylindrical handles etched on a dielectric substrate represents a wideband G-CSRR (WG-CSRR) unit cell in Fig. 5(a). This unit cell has four via interconnects forming a 4-port network, through which the collected power is gathered and delivered to the RF combining network as shown in Fig. 5(b). Compared to G-CSRR, the achieved beamwidth of the WG-CSRR array is almost 4.5 times wider. The authors in [24] proposed an adaptable ultra-thin curvature metasurface-based WEH system at 5.33 GHz. The designed harvester, a sample of which is depicted in Fig. 6, is composed of 11 × 11 complementary quad SRR (CQSRR) unit cells on Rogers RO3010 PCB with copper thickness of 17 μm. Results show that the proposed system achieved an EHE of up to 86% for normal radiation, and became 72% and 62% for 70° oblique angle of incidence from H-, and E-plane, respectively.

In [25], the authors designed a metasurface structure of dimensions 15.7 × 15.7 mm^2 comprising 9 × 9 electrically small square-ring resonator subwavelength unit cells, which achieved an ECE of over 80%. Similarly, a 64-unit cell energy receiving adapter based on metasurface resonator, with each cell constructed of two face-to-face split rings that share the same gap was proposed in [26]. The designed adapter yielded an overall 86% RF-to-AC power reception efficiency and 78% AC-to-DC conversion efficiency. In a subsequent demonstration, the authors also proposed a 13 × 13 unit cells metasurface energy harvester whose design was realized on a dielectric substrate with a ground plane. The conductive layers of the top and bottom sides are connected to the load through vias while adjacent elements of unit cells are spaced 0.25 mm apart and each unit cell is attached with an 82 Ω resistor. Measured and simulated results at 3 GHz revealed that 93%, and 97% EHE, was attained respectively.

TABLE 2. Summary of related works on metasurface structures for WPT and WEH.

Ref.	Frequency (GHz)	Substrate material	Metasurface structure	No. unit cells (Periodicity)	RF–DC Efficiency (%)	Requires Matching Network?
[21]	5.8	RT5880	Split Ring Resonator (SRR)	9×9 ($0.199\lambda_o$)	50–75%	Yes
[22]	5.55	RT5880	Ground-backed Complementary SRR (GC-SRR)	11×11 ($0.34\lambda_o$)	92%	Not required
[23]	5.6	RO4003	Wideband GC-SRR (WGC-SRR)	9×9 ($0.045\lambda_o$)	93%	Yes
[24]	5.33	RO3010	Complementary Quad SRR (CQSRR)	11×11 ($0.13\lambda_o$)	73.7%	Not required
[25]	2.5	F4B	Closed Square-Ring Resonant	9×9 (λ_o)	80% @ 5.8 GHz; 85.1% @ 2.57 GHz	Yes
[26]	2.45	RO4350B	SRR	8×8 (λ_o)	78%	Yes
[27]	5.80	RT6006	ELC	9×9 (λ_o)	95%	Yes
[28]	2.45 & 6	RT6006	Pixelated Metasurface	9×9 (λ_o)	95% @ 2.45 GHz; 90% @ 6 GHz	Yes
[29]	2.45	TMM10	Fractal Cell	9×9 ($0.123\lambda_o$)	96.5 %	Yes
[30]	2.0	RO4003C	Dipole-Embedded Ring Super Cell	2×2 (λ_o)	98%	Yes

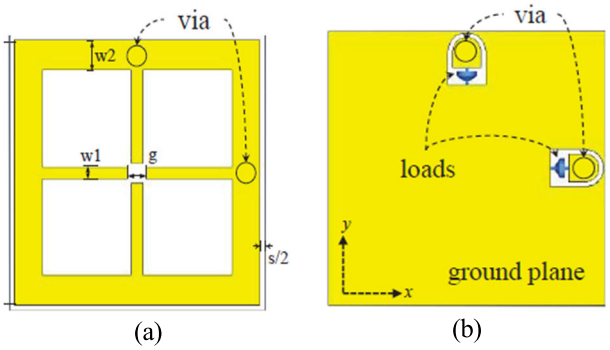

FIGURE 7. Schematic of symmetric ELC resonator: (a) top view; (b) bottom view [27].

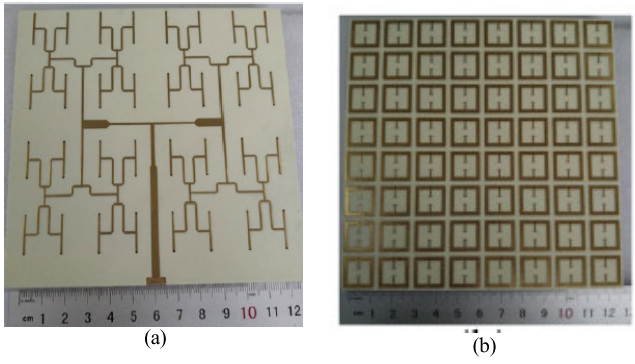

FIGURE 8. (a) Corporate feed network with edge feeding in [26]; and (b) top layer 8 × 8 metasurface cells.

Besides SRR and its variants, metasurfaces can be created from arrays of meta cells of other shape structures. The authors in [27] presented the design of a polarization-insensitive 9 × 9 cells electric-inductive-capacitive (ELC) resonator at 2.45 GHz for WEH applications. The ELC resonator sample has two vias connected with two resistors, as shown in Fig. 7, and achieved ECE of more than 92% for different polarization angles (0−90°). Similarly, a dual-band polarization-insensitive metasurface energy harvester composing of an array of pixelated unit cells is proposed in [28]. Yet another polarization-independent but fractal-based metasurface is proposed in [29] for IoT applications, offering a very compact design, high absorption coefficients, and an EHE of 96.5%. In [30], the authors designed a dual polarized metasurface based on an array of super cells each formed by four dipole-embedded rings for energy harvesting. Unique to this design is the absorbed power being mostly dissipated across a resistive load rather than within the dielectric substrate. It yielded a power absorption efficiency of 98% and a radiation to AC efficiency of around 98% for each polarization.

Table 2 summarizes the designs and performances of the metasurface structures covered in this subsection.

B. FEED NETWORK

As metasurface unit cell array needs to be tightly spaced to achieve good impedance balance, it is impossible to include the feed network on the same surface where these arrays of

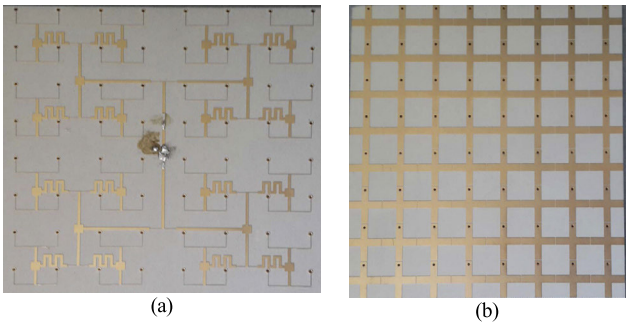

FIGURE 9. (a) Corporate feed network with inset feeding in [33]; and (b) top layer 64-cell ERR metasurface.

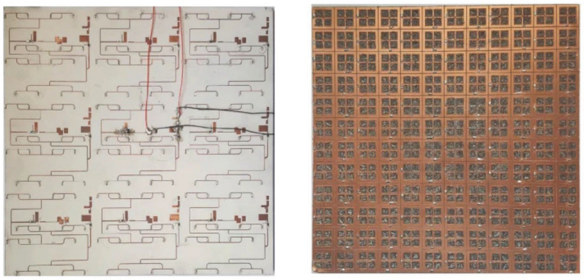

FIGURE 10. (a) Corporate feed networks (two per super cell) with on-board rectifiers in [34]; and (b) top layer with nine super cells (total 144 unit cells).

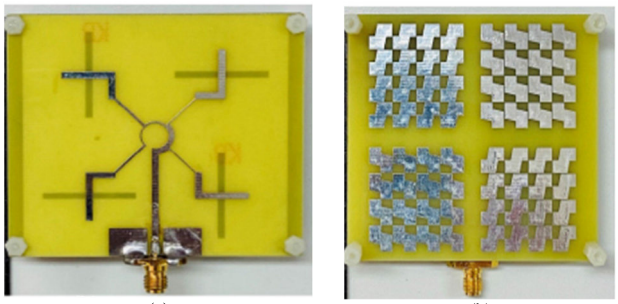

FIGURE 11. (a) Sequentially-rotated feed network with edge feeding in [35]; and (b) top layer with four 4 × 4 S-shaped cell clusters.

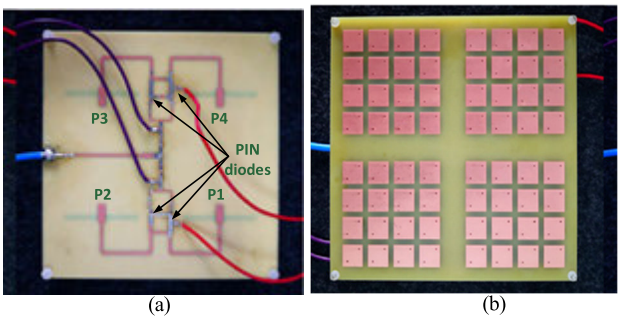

FIGURE 12. (a) Corporate feed network with edge feeding and PIN diodes for reconfiguration of propagation mode in [36]; and (b) top layer with four 4 × 4 sub-arrays.

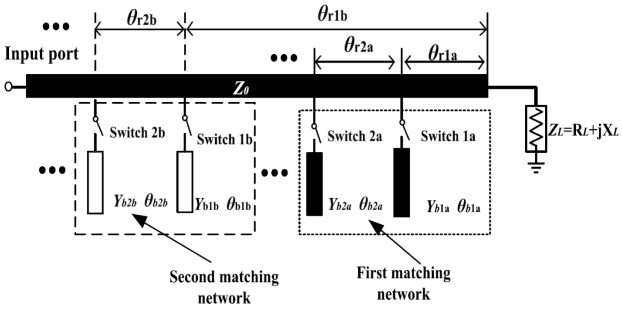

FIGURE 13. The topology of a wideband reconfigurable IMN for dual-band operation (two switchable stubs for each operating band) proposed in [38].

unit cells are positioned. This is contrary to the conventional patch array that has wider spacing between adjacent antenna elements, providing sufficient room to house both feed network and antenna elements on the same copper plane. Thus, for a metasurface structure, an additional conductive layer is required to host the feed network. The main purpose of the feed network is to channel the overall energy collected by the unit cell array to a target load. There are different feed network designs, which can be generally categorized into series-feed, corporate-feed, or corporate-series feed. The series and corporate feed networks use single, and multiple transmission lines, respectively, to connect all unit cells to a terminal port, whereas corporate-series feed uses a combination of both approaches.

While arrays can be fed by any of these methods, series feed and corporate feed remain the two most widely used feed techniques. Although the design and fabrication of series feed network can be simpler than corporate feed network, series feed has an issue of high voltage standing wave ratio (VSWR) arising from additive misalignments at connections between elements, as well as the drawback of progressive phase delay between them. For these reasons, series feed is less suitable for phase scanning and for structures with large footprint such as metasurfaces [31]. On the other hand, the corporate feed network offers more flexible control over the functionality of each unit cell, making it more suitable for phase scanning and beam shaping and thus preferable for metasurfaces. Figs. 8-12 depict various fabricated feed networks along with their corresponding metasurface energy harvesting structures.

In [26], a feed network (also referred to as RF combining network) using corporate feed technique and impedance transformers is implemented on a second layer on the underside of the top layer that hosted 8 × 8 unit cells to channel the collected RF power to a single load for RF-to-DC conversion, as shown in Fig. 8. Each terminal of the elementary scattering particle is connected to the feed network by means of vias and terminated with 90 Ω impedance. The metasurface achieved a total reception efficiency of 67% and a peak AC-to-DC conversion efficiency of 78% at a resonant frequency of 2.45 GHz under a total input AC power level of 10 dBm.

In [33], a hypothetical 64-element energy harvesting panel is used to illustrate the importance of feed network in metasurfaces. Since no feed network is used for channeling AC power of all the unit cells to a single resistive load in this hypothetical scenario, the constitutive 64 unit cells are

TABLE 3. Summary of related works on feed networks for metasurfaces.

Ref.	Frequency (GHz)	Number of unit cells	Termination impedance (Ω)	Feed network configuration
[26]	2.45	8×8	90	Corporate feed with impedance transformers
[33]	2.82	8×8	300	Corporate feed with three transmission lines of different characteristic impedances for constructive signal combination at rectifier input
[34]	2.4	9×8×2	175	Two three-stage corporate feed networks, each for one orthogonal polarization of a super cell metasurface
[35]	4.0–9.0 & 4.2–7.6	4×4×4	50	Sequentially-rotated feed network consisting seven λ/4 transformers with differential characteristic impedances
[36]	6.2	4×4×4	90	Reconfigurable corporate feed network using four-way switchable power divider loaded with PIN diodes to realize two helical propagation modes for a metasurface antenna array

individually terminated with a rectifying diode, enabling each element to convert its own intercepted incident RF energy to a DC voltage, assuming that all elements have unity efficiency. Thus, the number of diodes in the configuration is equal to the number of the constituent unit cell particles of the metasurface panel. This leads to several issues: (i) reduced power density available per diode since each diode receives a fraction of the incident power; (ii) longer diode turn-on time; (iii) higher system cost for metasurfaces with larger footprint; and (iv) AC-to-DC conversion losses could increase linearly with the number of diodes. Consequently, the same authors designed a corporate feed to combine the RF output power of their proposed 64-cell metasurface, which is constructed of 8 × 8 electric ring resonator (ERR) adaptors. As shown in Fig. 9, three transmission lines of different widths were used to realize different characteristic impedances for matching to a 50 Ω load. The feed network matched the input impedance of the unit cells to the load such that it resulted in constructive combination of signals at the rectifier input. The achieved total radiation to DC conversion efficiency was over 40% at a working frequency of 2.82 GHz under the input power level of 12 dBm.

In [34], two corporate feed networks, each for one orthogonal polarization of a super-cell metasurface for RF energy harvesting is presented as shown in Fig. 10. Each super cell consists two groups of eight unit cells, one per polarization, from which the collected AC power is combined in three stages through the two feed networks. The cells are connected to their feed networks on the bottom layer through via-holes, and terminated with lumped impedance of 175 Ω. At a resonance frequency of 2.4 GHz, the proposed structure channeled and converted ∼70% of the harvested energy to DC power with an input power of ∼9 dBm. It is important to note that the AC losses of the feeding circuit, particularly for large-footprint structures, can be significant, which in turn can make it difficult to achieve high energy conversion efficiency.

The sequentially-rotated feed network proposed in [35] was not specifically designed for RF energy harvesting, but its design that consists of seven λ/4 transformers with different characteristic impedances offers a design insight of an efficient feed network for RF energy harvesting. The proposed feed is attached to four 4 × 4 S-shape cluster metasurface as shown in Fig. 11. Experimental results show that the proposed structure could achieve phase quadrature with equal magnitude, axial bandwidth of 84.74% at 4–9 GHz and 57.6% at 4.2–7.6 GHz, for a center frequency of 5.9 GHz.

In [36], an efficient, but unconventional reconfigurable corporate feed network was proposed. As depicted in Fig. 12, it encompasses a four-way switchable power divider loaded with PIN diodes. RF signal is excited at the feed point, divided into four sub-signals by the switchable power divider and transferred to four ports through transmission lines. The feed is then applied to a circularly polarized metasurface composing four 4 × 4 sub-arrays operating at 6.2 GHz with two helical propagation modes (clockwise; anti-clockwise) reconfigurable through the PIN diodes in the feed network. Although this feed network was applied to operate in transmit mode, its underlying design philosophy and high efficiency also make it an attractive candidate for WEH as an RF combiner that channels the collected energy from the metasurface to a rectification circuitry.

Table 3 summarizes the discussed works on feed network for metasurfaces in this subsection.

C. IMPEDANCE MATCHING NETWORK

A well-designed impedance matching network (IMN) is critical to preventing standing waves and ensuring maximum transfer of power between different stages in the RF system. It is still challenging to design an accurate IMNs for RF energy harvesting systems, particularly if there is a need for the harvester to operate over a wide range of input power, a wide range of loads, and across multiple frequency bands.

An adaptive IMN that operates over a wide range of input power for a rectifier system was proposed in [37]. The input power was divided into subranges, each having a specific matching circuit designed. Since output voltage varies with input power, the appropriate matching circuit is selected using switches based on feeding a fraction of the output DC voltage to control the switches. Due to single frequency operation, simple matching circuits based on single short-circuited stub circuits were used. For a case of two subranges centered at 0 dBm and 15 dBm, up to 20% improvement in RF-to-DC

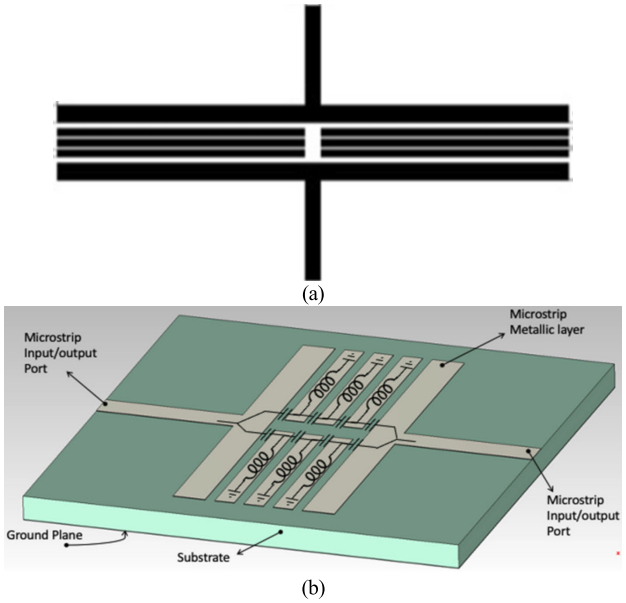

FIGURE 14. (a) Layout of the metamaterial IMN; and (b) its equivalent circuit model proposed in [39].

conversion efficiency is obtained for input power ranging from −5 to 20 dBm.

A wideband reconfigurable IMN was proposed in [38], which comprises one transmission line and two switchable stubs for each operating band as shown in Fig. 13. The stubs can be open or short circuited, while switching can be performed using PIN diodes or MEMS switches for low, or high frequencies, respectively. The electrical lengths of the transmission line and stubs are optimized to achieve wideband matching at multiple frequency bands, while meeting the minimum desired return loss in the band of interest. Unlike conventional reconfigurable IMN with single stub tuners, the proposed IMN is also capable of matching over a wide range of load impedances. Two dual-band prototypes with working frequencies between 1−3 GHz were presented to match different complex loads at different frequency bands.

Metamaterials offer a high degree of freedom in designing transmission lines, making them possible to achieve impedance matching across multiple bands. In [39], a metamaterial IMN formed by symmetric rows of capacitively coupled λ/2 microstrip resonators was proposed as shown in Fig. 14. The stub parameters of the resonators are optimized to minimize the S_{11} at the λ/2 resonant frequencies (S_{11} = 0 indicates aperfect match). The proposed IMN was fabricated and utilized for matching a WiFi antenna to a bridge rectifier of an ambient energy harvesting system operating at multiple bands of around 2.4 GHz and 5 GHz.

Similarly, an IMN based on two-dimensional metamaterial, i.e. metasurface, was proposed in [40] for matching the impedance of an antenna to that of a RF front-end circuitry. The metasurface IMN was constructed of rectangular spirals and metallized via-holes, behaving as left-handed series capacitances, and shunted inductances, respectively,

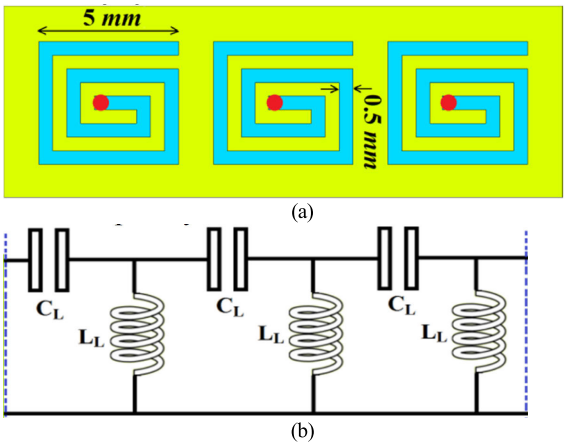

FIGURE 15. (a) The schematic design of the metasurface IMN; and (b) its equivalent circuit model proposed in [40].

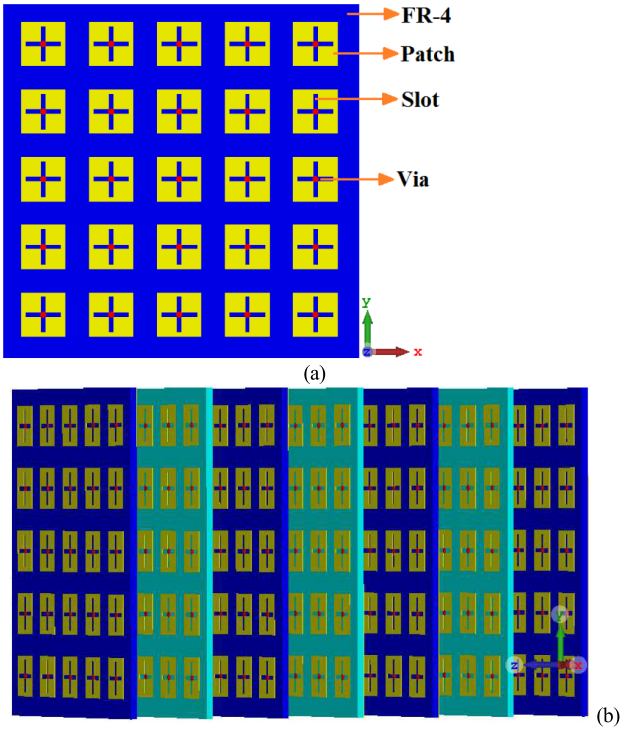

FIGURE 16. (a) The schematic design of a metasurface as impedance matching sheet; and (b) stacked metasurface sheets as IMN proposed in[41].

as shown in Fig. 15. It overcomes the gain-bandwidth limitations of traditional method of matching using discrete components. Results show that the proposed IMN can be applied to electrically small antennas at working frequencies of 1.4 GHz and 1.75 GHz with low loss.

The authors in [41] realized an IMN to reduce the impedance mismatch between a receiving antenna and free space by stacking metasurface sheets as shown in Fig. 16. A metasurface sheet comprises an array of unit cells with subwavelength periodicity, each consists of a square patch with cross-shaped slot grounded through a via-hole. The patch and the via constitute the series capacitance, and shunt

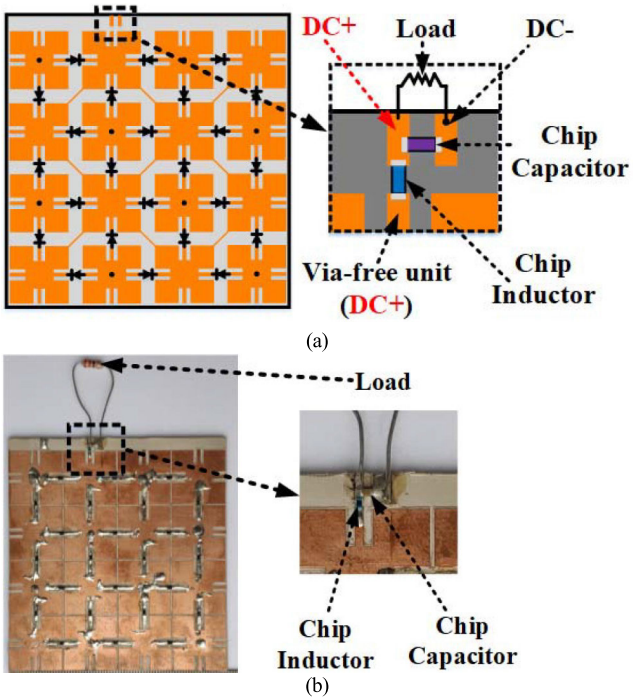

FIGURE 17. (a) The schematic design; and (b) fabricated prototype of the metasurface proposed in [14].

inductance of an LC resonant structure, respectively. Using the proposed metasurface sheets improved antenna's performance in terms of return loss, gain, and radiation efficiency across its operating frequency range between 3−5 GHz.

In [42], another IMN was presented for matching an electrically small magnetic loop antenna to the power source impedance at 450 MHz using a mu-negative (MNG) metamaterial hemisphere. MNG is the property of a material exhibiting negative permeability. The hemisphere is fabricated as an assembly of stacked spiral cells implemented on alumina substrate. Measurements show a 17 dB increase in total radiated power over an unmatched loop. However, this is lower than the 30 dB anticipated by the authors, which is attributed to losses in the MNG hemisphere.

Although, IMN is an important design aspect of rectenna systems, metasurfaces designs for RF energy harvesting have evolved in more recent times to eliminate the need for IMN by engineering near-perfect matching between the metasurface and adjacent impedances. For example, the authors in [14] realized an RF energy harvesting system that incorporated rectifying diodes directly onto the metasurface as shown in Fig. 17. The proposed metasurface comprises uniplanar compact photonic bandgap (UC-PBG) unit cells, which exhibit multimode resonance and adjustable impedance characteristics. This allows it to eliminate the IMN, resulting in a more compact size. Likewise, the authors in [43] engineered an RF energy harvesting metasurface whose impedance matches that of free space, enabling it to capture the impinging RF energy with minimum reflection. The metasurface comprises unit cells featuring metallic mirrored split ring resonators and hollow cylinders, as shown in Fig. 18. The equivalent circuit

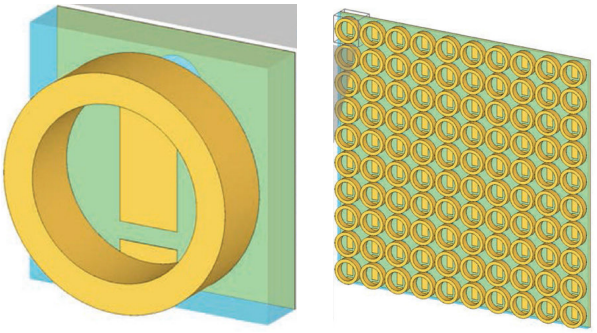

FIGURE 18. (a) The unit cell comprising a hollow cylinder structure and split ring underneath; and (b) array of unit cells in the metasurface proposed in [43].

of each unit cell operates as a matching network between free eachunit cell operates as a matching network between free space with impedance of ∼377 Ω and a 50 Ω output port.

Table 4 summarizes the IMN-related works discussed in this sub-section.

D. RECTIFIER CIRCUIT

A rectifier circuit with high RF-to-DC power conversion efficiency and the ability to generate sufficient DC voltage from weak received RF fields is challenging to design. The rectifiers for metasurfaces employed for RF energy harvesting can be realized using various circuit topologies.

In [34], a rectifier system for a super-cell metasurface harvester to convert energy from orthogonally polarized 2.1 GHz RF signals to DC power was designed. The system comprises two rectifier circuits, one per signal polarization. Each rectifier circuit features a Schottky diode and seven transmission line segments for impedance matching between diode, super-cell, and load. The two rectifiers have identical circuit layout but different transmission line dimensions. Experimental results show a maximum radiation to DC conversion efficiency of 70% is achieved at an input power of 9 dBm.

In [44], the authors proposed a two-sided metasurface consisting of modified ELC unit cells designed to resonate at 2.45 GHz on one side, and a rectifying circuitry on the other. The latter uses a voltage-doubler rectifier for each cell to directly rectify the received RF signal. The rectifier comprises a pair of series and parallel Schottky diodes, each connects to a capacitor using a microstrip line section. For a metasurface composing of multiple cells, the DC lines from each rectifier would then merge and connect to a load as shown in Fig. 19. The measured results show that a maximum RF-to-DC conversion efficiency of 76.8% is achieved at an input power of 0.4 dBm.

The authors in [14] introduced a single-shunt-diode rectifier with multichannel parallel connection for a rectifying metasurface as shown in Fig. 20. The diodes are parallelly connected to the energy harvesting ports between unit cells, whose impedances are directly matched to that of the rectifier at the desired frequency band. Different diode types could

TABLE 4. Summary of related works on impedance matching.

Ref.	Frequency (GHz)	RF input power	Impedances matched	Matching type and configuration
[37]	2.45	–5 to 20 dBm	Varying rectifier impedance with RF input power	Adaptive IMN for antenna-rectifier matching; switch between matching circuits based on RF input power; use simple short-circuited stubs as matching circuits
[38]	1 & 1.75 1.25 & 2.75	N/A	$100 + j60\ \Omega$ $15 - j10\ \Omega$	Wideband reconfigurable IMN; comprises one transmission line, two switchable stubs for each operating band; dimensions optimized for wideband matching and minimum return loss
[39]	2.4 & 5	−30 dBm (ambient RF)	32 kΩ	Metamaterial IMN for antenna-rectifier matching; comprises rows of λ/2 microstrip resonators with dimensions optimized to minimize S_{11} at resonant frequencies
[40]	1.4 & 1.75	N/A	N/A	Metasurface IMN for antenna-RF front-end matching; constructed of rectangular spiral resonators and via-holes;
[41]	3–5	N/A	377 Ω (free space)	Stacked metasurface sheets IMN for antenna-free space matching; unit cell comprises a square patch with cross-shaped slot grounded through a via-hole
[42]	0.45	N/A	50 Ω (source)	Mu-negative metamaterial hemispherical IMN for magnetic loop-power source matching; constructed as an assembly of stacked spiral cells on alumina substrate
[14]	2.4 & 5.8	–3 to 10 dBm	700 Ω	Direct metasurface-rectifier matching; comprises a co-planar design of integrated diodes and UC-PBG unit cells; exhibit multimode resonance and adjustable impedance characteristics
[43]	2.45	N/A	377 Ω (free space)	Direct metasurface-free space matching; comprises unit cells, each featuring a split ring and hollow cylinder

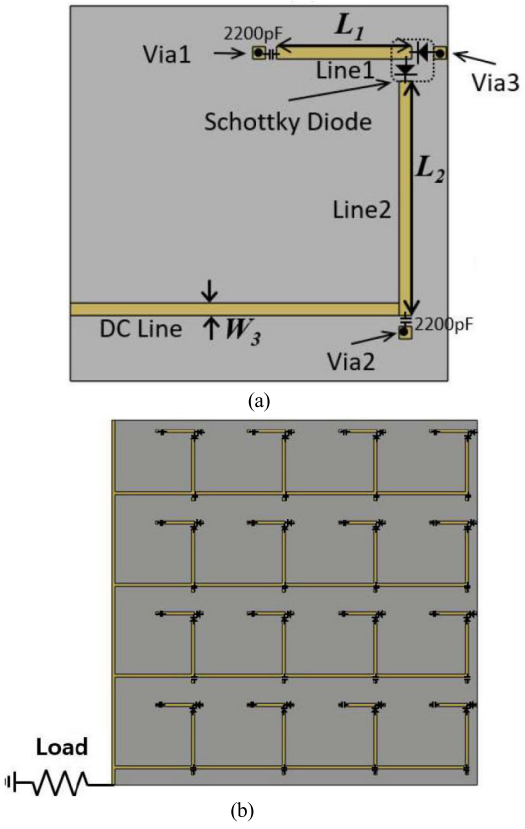

FIGURE 19. (a) Rectifier on the backplane of a unit cell; and (b) Inter-connected rectifiers for a 4 × 4 rectifying metasurface proposed in [44].

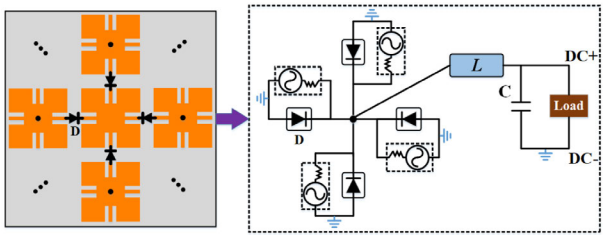

FIGURE 20. Schematic and equivalent circuit of one part of the rectifying metasurface proposed in [14].

be employed according to the expected input power without changes to the rectifier topology. The RF-to-DC conversion efficiency is found to reach 58% and 50% at 2.4 GHz, and 5.8 GHz, respectively, with an input power of 0 dBm.

In [45], the authors presented a half-wave rectifier for a metamaterial-integrated high-gain rectenna operating at 2.45 GHz. The rectifier comprising a Schottky diode, shunt-capacitor low-pass filter, and resistive load, is designed as a separate layer of a three-layer rectenna structure. Both capacitor and resistive load values are optimized to achieve maximum RF-to-DC conversion efficiency at an input power of 10 dBm. The resulting component values gave a low-pass cut-off frequency of 1.45 MHz and RF-to-DC conversion efficiency of up to 78.9%.

The authors in [46] presented a 2.45 GHz rectifying metasurface with integrated rectifiers, one for each unit cell. Each rectifier employs a Schottky diode connecting the unit cell through an optimally placed via where circulating currents merge to achieve optimal energy delivery and impedance matching. Moreover, the rectifiers are shielded by a metallic ground layer from interference by high power incident EM waves. As shown in Fig. 21, the rectifier comprises an inductive microstrip line that connects the via, diode and blind via.

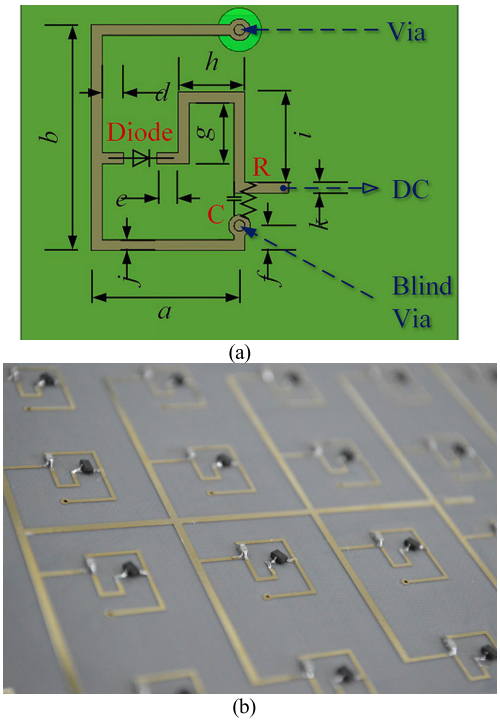

FIGURE 21. (a) Schematic of the rectifier for each cell; and (b) Fabricated rectifiers for an array of unit cells of the rectifying metasurface proposed in [46].

It suppresses the diode's reactance while matching its resistance to that of the unit cell. Another microstrip line connects to a capacitor working as a low-pass filter that outputs a DC voltage to a resistive load. The measured results showed a RF-to-DC conversion efficiency of 66.9% is achieved under an incident power density of 5 mW/cm^2.

Table 5 summarizes the related works on rectifier circuits for metasurfaces discussed in this subsection.

E. METASURFACES VS RELAY FOR NLOS POWER TRANSFER

RF propagation environments can be repleted with obstacles that block line-of-sight (LOS) signals. In most cases, a transmitted RF energy-bearing signal has to circumvent these obstacles to arrive at the receivers. A possible mitigation to the RF obstruction issue is to sense the environment and identify in real-time an alternative propagation path to deliver the energy-bearing signal to receivers without compromising the power level. In this situation, an established method is to deploy relay stations [47], which can turn a non-line-of-sight (NLOS) link into multiple LOS links, as illustrated in Fig. 22(a). However, this requires that each relay must be equipped with a relatively high-capacity power source and necessary front-end circuitry for reception, processing, and re-transmission of RF signals. For this reason, the use of relays may increase network power consumption and capital expenditure for deployment [45].

On the other hand, metasurfaces can transform the unpredictable propagation environment into a programmable and partially deterministic space by having metasurfaces strategically mounted on signal-blocking obstacles, thereby converting them into programmable smart surfaces. These smart surfaces have the unique ability to spatially amplify the signal strength in propagation and to re-direct the signal propagation to the locations of non-LOS UEs while enhancing energy reception and end-to-end power delivery efficiencies at much lower implementation costs (see Fig. 22(b)).

Subsequently, metasurfaces can be deployed as a strategy to smartly navigate through obstacles in the near-field scenarios. The authors in [48] have analyzed the influence of dielectric and metallic obstacles on the performance of a metasurface-based WPT system in an indoor near-field environment. They explored the capabilities of a smart table made of metasurface in which multiple UE energy receivers are set to be charged simultaneously. Both transmitter and receivers are placed on top of the smart table, and a ceramic dielectric obstruction is placed in between. The same experiment is established for a copper metallic obstruction with the same geometric parameters. The results show that an overall WPT efficiency of 90% is achievable over a distance of 80 cm between the transmitter and receivers, and that the presence of dielectric and metallic obstructions do not significantly diminish the WPT efficiency because of the surface mode localization and symmetry.

Besides metasurfaces and relays, another method that has been used to establish alternative routes in the presence of physical obstructions or when the quality of LOS path is insufficient is to utilize passive non-reconfigurable specular reflectors [49], e.g., dielectric or metallic mirrors. Like metasurfaces, this coverage improvement strategy has the advantage of low cost compared to active relaying, particularly in high-frequency bands. Nevertheless, a fundamental drawback of non-reconfigurable specular reflectors arises from their inability to enable dynamic molding of the incident waves since their operation cannot be adjusted after manufacturing. Because of the profoundly dynamic nature of the RF propagation environment, it would be useful for such reflectors to have the ability of shaping RF waves according to the obstacles and environmental conditions. Some differences between the use of metasurfaces and relays in WPT have been expounded as follows.

1) IMPLEMENTATION COMPLEXITY

The use of relay stations is a well-known strategy for transferring energy signals from a transmitter to energy receivers at remote or non-LOS locations [45], [49]. However, such relays are typically seen as active systems that need a high-capacity power source for operation. They are furnished with active components such as mixers, analog-to-digital converters (ADCs) and low-noise amplifiers for signal reception, and digital-to-analog converters (DACs) and power amplifiers for signal relaying. Furthermore, to maximize the rate-energy transfer efficiency, additional components are needed for implementing decode-and-forward (DF) and amplify-and-forward (AF) relaying. Thus, the implementation of relays

could be costly and power-consuming, especially when realizing a multi-antenna design and operating at high mmWave and Terahertz frequency bands where signals would experience high propagation loss [50].

In contrast to active relaying, the configurability of metasurfaces can be realized through inexpensive, low-power and low-complexity components (switches or varactors) [51], which make them more suitable than relays for large-area implementation and mass production. Thus, the implementation complexity could be addressed by replacing the active relays with intelligent metasurface structures.

2) POWER CONSUMPTION

In contrast to relays that need high-capacity power sources for transmission and operation of their active components, reconfigurable metasurfaces could be deployed in near-passive implementations as only low-power active components such as switches and varactors are required, making metasurfaces a suitable technology for realizing large-scale and power-efficient WPT and WEH systems.

In active relay systems, the total RF power is often allocated between the transmitter and the relay to ensure that the overall power consumption is within a given power budget. This is unlike in metasurface systems where the transmitter gets to utilize the total RF power. The amount of energy reflected by a metasurface depends on the power density of the impinging radio wave, which can be maximized through an appropriate design of the metasurface structure.

F. POWER LOSS IN PRACTICAL METASURFACES

There are several factors that contribute to power loss in practical metasurfaces for WPT and WEH applications, making it strenuous to attain a unity power conversion efficiency. One of the common factors is the reflection power loss due to non-zero energy dissipation of the impinging incident wave in each element of the metasurface caused by imperfect hardware with non-negligible dielectric, metallic, and ohmic losses. This leads to the reflection coefficient of each metasurface element to be less than unity. Moreover, in metasurfaces with reconfigurable reflection phase for beamforming applications, the amplitude of this reflection coefficient varies non-linearly with its phase shift, resulting in non-uniform reflection power loss [32].

Another common factor is the signal reflection between the metasurface structure and its feed cable. For instance, in the double-fed unit cells architecture proposed in [52], where a series of cascaded radiating meta cells are integrated with non-reciprocal phase shifters, the power loss observed in this setup was due to the reflection between the metasurface structure and the feed cables. It was shown that each transmitting double-fed unit cell introduces more than 6 dB radiation loss, leaving about 75% of the power injected into the left feed-line of the unit cell re-radiated into the air. The remaining 25% of the power is transmitted to the feed-line in the right-hand side of the unit cell.

Consequently, the wide impedance bandwidth response offered by the feed gap of metasurface unit cells can be exploited to eliminate the impedance matching network between the metasurface particles and the rectifying diode, which would not only reduce the footprint of the metasurface, but also the power losses that could have been introduced by the matching network. To realize this approach, the authors in [53] placed a pair of 100 nH SMT L-14CR10JV4T inductors on both sides of each diode to filter out the harmonic signal and pass the DC rectified power, which is then channeled to the load directly without a matching network. Nevertheless, the inductors still introduced some power loss, resulting in a radiation to DC conversion efficiency of over 80%.

Power loss in practical metasurfaces has also been attributed to the number of layers constituting the metasurface structure, with single-layer metasurfaces particularly prone to power loss. In [54], a single-layer circularly polarized metasurface is proposed, which can modulate the phase shift in two perpendicular directions in a way similar to the traditional dielectric polarizers. However, this single-layer metasurface suffers half power loss, i.e. it reflects 50% of the power of the incident linearly polarized wave and converts the other 50% into useable DC power. To mitigate this power loss problem, it was modified to become a multiband absorber by stacking extra layers of metallic and dielectric of different thicknesses on top of the existing structure. However, it should be noted that each of these additional layers may also introduce its own power loss to the system.

The energy harvesting metasurfaces presented in [33], [44] all require additional layers to host the RF combining circuit due to the tight coupling of the metasurface elementary particles. The feed circuit collects the AC power from each elementary particle (i.e., unit cell) prior to rectification and then fed it to a single rectifier circuit. The feed circuits are prone to incurring losses that affect the overall frequency bandwidth response, and by extension the RF-to-DC conversion efficiency of the system.

As could be seen above, minimizing the power loss in practical metasurfaces is a multi-faceted problem, which remains an open research challenge that requires further investigations.

IV. APPLICATIONS TO EMERGING TECHNOLOGIES FOR FUTURE NETWORKS

This section discusses the applications of metasurface-aided WPT and WPE systems to emerging technologies for future wireless networks, namely WPCN, SWIPT, and mmWave. This will offer the opportunities to enhance the power transfer and energy harvesting efficacies, and therefore allow low-power UEs to generate sufficient output energy from incoming RF signals to charge their on-board batteries for sustained operation in future networks.

TABLE 5. Summary of related works on rectifier circuits.

Ref.	Frequency (GHz)	RF-to-DC efficiency	Input power/ power density	Rectifier type and circuit topology
[34]	2.1	70%	9 dBm	Two rectifier circuits, one per signal polarization; each featuring a Schottky diode and seven transmission line segments of different dimensions
[44]	2.45	76.8%	0.4 dBm	One voltage-doubler rectifier per cell; comprising a pair of series and parallel diodes, each connects to a capacitor using a microstrip line
[14]	2.4 5.8	58% 50%	0 dBm	Single-shunt-diode rectifier where diodes are parallelly connected to harvesting ports and directly matched to impedance of the metasuface
[45]	2.45	78.9%	10 dBm	Half-wave rectifier comprising a Schottky diode, shunt-capacitor low-pass filter, and load optimized for maximum RF-to-DC conversion efficiency
[46]	2.45	66.9%	5 mW/cm^2	One integrated rectifier per cell; comprising a Schottky diode and two microstrip lines that connect the diode to a via/blind via and low-pass filter; the vias are optimally placed to achieve good impedance matching and energy delivery

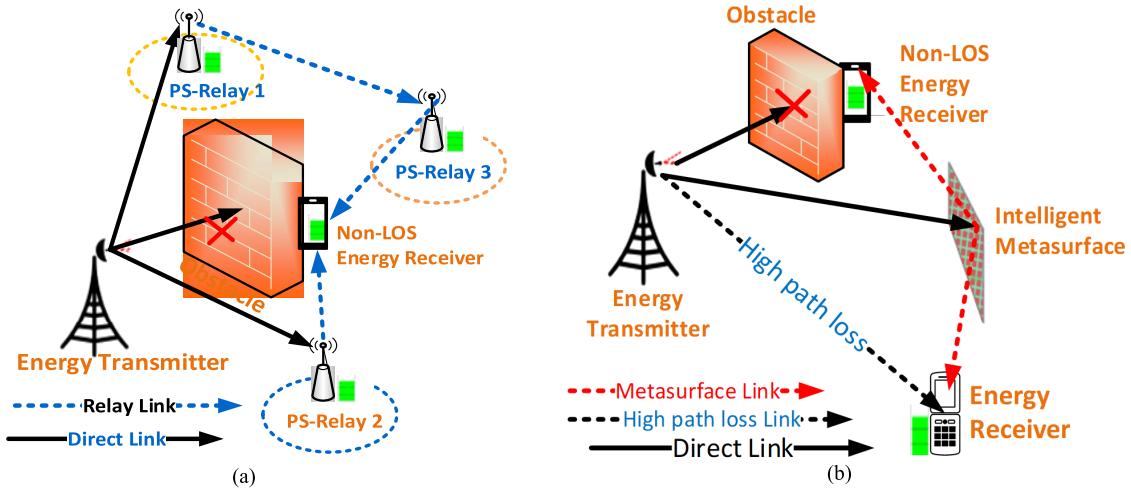

FIGURE 22. Cooperative networks: (a) Relay aided transmission based on power splitting (PS) scheme; and (b) Metasurface aided transmission.

A. WPCN

In [55], the authors proposed a hybrid-relaying scheme for WPCN, which uses a metasurface as an intermediate node to relay the downlink (DL) energy from dedicated energy transmitters to UEs, and the uplink (UL) information from UEs to the HAPs. In [56], an intelligent reflecting surface (IRS), which can be implemented using metasurfaces, is used to enhance DL energy transfer and UL information transfer in a cooperative WPCN. Moreover, IRS phase shifts, transmit time and power allocations are jointly optimized to maximize throughput of the cooperative transmissions. The authors in [57] considered the energy minimization problem in an IRS-aided WPCN, where IRS assists the energy transfer from a dedicated energy station (ES), and information transfer to a data sink using non-orthogonal multiple access (NOMA). Moreover, the IRS phase shifts and transmit resource allocation are jointly optimized to minimize the energy consumption of the ES.

In [58], the authors jointly optimized radio resource allocation and passive beamforming for a reconfigurable intelligent surface (RIS) assisted WPCN to improve the system energy efficiency. The system operates a harvest-then-transmit (HTT) protocol where users harvest energy from a dedicated ES with the aid of RIS and then transmit their information to a receiver via a time division multiple access (TDMA) scheme. Note that RIS is alternatively referred to as IRS in literature, which similarly can be implemented using metasurfaces.

These are different ways of integrating metasurfaces with WPCN, which although is a promising network architecture for end-to-end energy delivery, its implementation and maintenance costs could be exorbitant that require huge capital investment [59]. For this reason, SWIPT is deemed as a more favorable alternative, since it is able to simultaneously carry energy and information in the same transmitted signal, eliminating the need for capital-intensive hardware such as dedicated energy transmitters.

B. SWIPT

Currently, the efficiency of SWIPT is constrained by issues of severe attenuation and randomness of wireless channels, leading to weak received power that can hardly activate

the energy harvesting circuitry of the SWIPT system. Furthermore, SWIPT demands much higher received power for energy harvesting than it does for information decoding. This imposes practical efficiency limitations on energy harvesting in SWIPT given the low power density that characterizes the wireless networks. Consequently, researchers have proposed the use of metasurfaces or metamaterials to increase signal propagation efficiency and by extension the received power levels [60].

In [61], the authors proposed a SWIPT network that leverages the high beamforming gain of a RIS to enhance the efficiency of wireless power transfer, thereby increasing the rate-energy trade-off performance. More specifically, several RISs are deployed to direct the propagation of energy-bearing signals towards non-LOS UEs. This approach showed an improvement of up to 80% in energy harvesting efficiency of SWIPT receivers when compared to the case of not using RISs. In [62], a SWIPT MIMO system is used with a IRS with reconfigurable phase shifts for enhancing both energy and information reception performances. The authors proposed a block coordinate descent (BCD) algorithm to jointly optimize the transmit power at the BS and phase shifts at the IRS. They showed a remarkable improvement in system rate-energy performance and rapid convergence of the proposed BCD algorithm, which is potentially beneficial for practical applications. In [63], the authors studied the transmit power minimization problem by jointly designing active and passive beamforming in a IRS-assisted SWIPT system. They performed an optimization of information-energy transmission at BS and beamforming at IRS to evaluate the minimum power level that can be received across all energy harvesters in the network.

C. mmWave

To alleviate the overcrowding of the microwave spectrum, mmWave has been advocated for use in future wireless networks. However, transmissions at mmWave frequencies incur high path loss due to atmospheric absorption, resulting in short transmission range that in turn increases their susceptibility to non-LOS obstructions. To address these issues, MIMO techniques are commonly used. However, this approach involves complex RF signal processing and requires sufficient spacing between antenna elements to minimize mutual coupling. This increases both the structure size and implementation cost. Consequently, researchers have proposed replacing MIMO antennas with metasurfaces [64], [65], which can realize spatial processing of energy beams without requiring amplifiers or active phase shifters, and thus efficiently transfer RF power to longer distances at lower costs.

In [66], the authors proposed a sectorized directional WPT scheme for IRS assisted mmWave network, where ES transfers energy to devices in selected charging sectors, and the IRS is deployed in each sector to achieve high passive beamforming gain and provide additional effective reflection paths to drastically enhance end-to-end energy delivery efficiency. In [67], a high-efficiency compact mmWave phased array for wireless energy transmission is proposed, in which metasurface technology is used for providing deterministic propagation paths for mmWave systems to overcome blockage and increase power transfer efficiency. The authors in [68] presented a mmWave RIS with electronically tunable metasurface. Using a capacitively-coupled patch parasitic resonator loaded with a PIN diode, a controllable two-state reflection phase with 180° phase difference is realized. Results showed that when used as a far-field reflector between two non-LOS users, a received energy gain of 25 dB is achieved over the reference case of a simple metal plate reflector. Unlike most metasufaces in literature, which can only manipulate the EM waves impinging one side, the authors in [69] presented the design of an anisotropic metasurface that can operate in reflection mode on one side, and transmission mode on the opposite side, at quasi-mmWave band of 28 GHz. This enables the metasurface to collect more energy from both front and rear sides than its single-sided counterparts. For instance, an optically transparent version of this metasurface can be installed on glass walls to collect and direct energy from both indoor and outdoor towards a target area or user for energy reception.

Table 6 summarizes the reviews on the applications of metasurface-aided WPT and WPE systems to emerging technologies for future wireless networks.

V. OPPORTUNITIES

Based on the preceding literature review, this section discusses a number of identified open research issues that also represent potential opportunities for future research. It further presents our proposed approach to leveraging metasurface technology holistically for optimizing end-to-end energy delivery in future wireless networks.

A. OPEN RESEARCH ISSUES

1) MMWAVE METASURFACES FOR WPT AND WEH

Existing works on mmWave metasurfaces have mostly focused on their utilization for enhancing the communication performance of mmWave wireless networks [70]. In contrast, research on metasurfaces for WPT and WEH at mmWave frequencies is still in its infancy. This is ostensible as they are non-trivial to design. Besides the well-known fabrication challenges, they have higher sensitivity to power loss compared to their microwave counterparts [71]. For instance, it has been shown in [72] that losses introduced by conductor irregularity could significantly impact the energy harvesting potential of a mmWave metasurface. Thus, further research is required to address these challenges.

2) LIMITED ENERGY GATHERING CAPACITY

The performance of metasurface rectennas (MSRs) can be significantly constrained by low available RF power density in their operating environments. Furthermore, most existing MSRs have small structural size. These twin factors of low RF

TABLE 6. Summary of related works on the applications of metasurface-aided WPT and WPE systems.

Ref.	Application	Problem addressed	Solution proposed	Limitations
[55]	WPCN	Path loss; low end-to-end energy delivery efficiency	Use metasurface as relay to enhance DL energy flow and UL information link	Metasurface itself needs to harvest sufficient energy to power its relaying operations
[56]		Weak energy transfer and cooperative transmission performance	Deploy IRS between HAP and users, and jointly optimize IRS phase shifts, transmit time and power allocations to maximize throughput of cooperative transmissions	Considered only a two-user cooperative scenario.
[57]		Minimize energy consumption of dedicated ES	Deploy IRS and NOMA to aid energy and information transfer, respectively, and jointly optimize IRS phase shifts and resource allocations to minimize energy consumption of ES	Requires a large number of IRS reflecting elements to avoid performance loss caused by imperfect channel state information (CSI)
[58]		Maximize system energy efficiency	Employ RIS to enhance energy transfer and jointly optimize radio resource allocation and passive beamforming to maximize system energy efficiency	Potentially high information transfer latency due to the use of the HTT protocol and TDMA scheme
[60]	SWIPT	Low energy and information delivery efficiency	Use IRS with SWIPT and a weighted sum power-information maximization scheme to improve energy-information delivery efficiency	Proposed scheme suffers from slow convergence rate
[61]		Non-LOS induced energy and information transmission loss	Employ RIS along with BS beamforming and RIS phase control schemes to maximize the minimum harvested power for a dual-hop communication scenario	Proposed schemes may require high receiver sensitivity
[62]		Poor energy and information receptibility in MIMO scenarios	Employ IRS and a BCD algorithm that jointly optimize BS transmit precoding and IRS phase shifts to maximize the weighted sum rate while meeting the energy harvesting requirement	Proposed algorithm not tested in real-world environments
[63]		Minimize transmit power at BS	Employ IRS and jointly optimize BS transmit precoding and IRS phase shifts to minimize BS transmit power, while satisfying user QoS constraints	Proposed scheme not tested in real-world environments
[66]	mmWave	Poor end-to-end energy delivery efficiency	Deploy IRS in sectorized fashion for directional WPT and jointly optimize BS transmit precoding and IRS phase shifts to maximize received power subject to energy harvesting constraints.	Incurs some energy loss due to high atmospheric absorption rate of the mmWave energy
[67]		Low radiation efficiency of general phased array	Design a metasurface-based compact phased array with serial-parallel feed to realize high radiation efficiency, low coupling between adjacent arrays and wide scanning angle.	Suffers low end-to-end energy delivery success rate in far-field setting
[68]		Non-LOS issue	Design and deploy a RIS with electronically tunable metasurface based on a capacitively-coupled patch parasitic resonator loaded with diode controllable two-state reflection phase	Slow beam steering speed. Requires faster switching components to increase beam steering accuracy
[69]		Low energy collection capacity	Design and deploy an anisotropic metasurface that harvests energy from both front and rear sides to enhance its energy collection capacity	High BS transmit power required to achieve good performance

power density and small structural size of MSRs have jointly placed a stringent limit on the energy gathering capacity, and by extension the RF-DC conversion efficiency of MSRs. Hence, current MSRs are only suitable for low-power devices such as wireless sensors. Innovations are required to enable high-capacity energy gathering.

3) LOW END-TO-END ENERGY DELIVERY EFFICIENCY

The literature on metasurfaces for WPT and WEH in wireless networks have mostly focused on their integration with energy transmitters and harvesters in isolation. While this may be viewed as a viable solution, it does not solve the issue of low end-to-end energy delivery efficiency prevalent in wireless networks. A more holistic approach by considering the different but complementary functions that metasurfaces play in this energy domain, i.e. their capability to manipulate RF energy transmission, absorption, and reflection, can enhance the network's end-to-end energy delivery.

4) FUNCTIONALLY RECONFIGURABLE METASURFACES

Due to the different functions that a metasurface can play, there will be different roles that a metasurface can perform in the delivery chain of WPT and WEH in a wireless network, e.g. as an energy harvester or reflector by manipulating the RF energy absorption and reflection characteristics, respectively. This leads to the desire of having a metasurface whose function can be dynamically reconfigured to adapt to changing energy needs in the network such as switching between being an energy harvester and energy reflector. Research on such agile metasurfaces is still in its infancy.

B. PROPOSED APPROACH

We propose to take a holistic approach to leveraging metasurface technology for optimizing end-to-end energy delivery in future wireless networks. We envisage a metasurface-aided wireless powered network (MWPN), where metasurfaces can interact with incident waves in a controlled adaptive manner, and UEs (not just low-power devices) can be powered by harvested RF energy. In this setting, metasurfaces are deployed as intermediaries to optimize both downlink energy and uplink information flows between BS/HAP and UEs. We also conceptualize a metasurface energy harvester-reflector (MEH-R) whose input section consists of

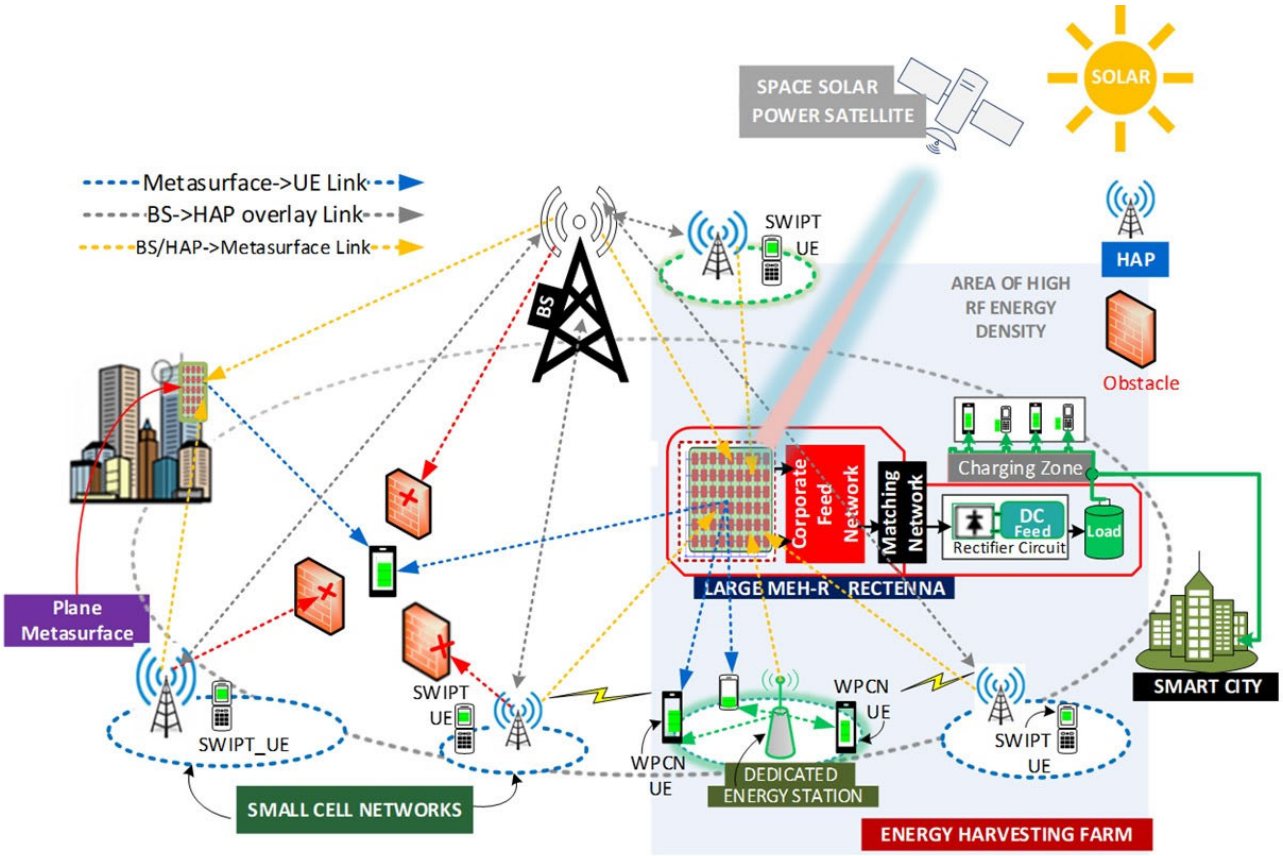

FIGURE 23. Proposed holistic approach to realizing a metasurface-aided wireless powered network.

a large-scale metasurface structure of one square meter or larger. In other words, we propose using two types of metasurfaces: planar metasurface as an intermediary; and MEH-R that can be dynamically reconfigured to function as an energy harvester or energy reflector.

Fig. 23 illustrates the proposed setting. MEH-R primarily performs RF energy harvesting, but can be reconfigured on-demand to reflect the incident RF signals to UEs within its vicinity. The reconfiguration from energy harvesting to energy reflecting only happens when the energy storage device of the MEH-R has been charged to its capacity. Then, the MEH-R can reflect energy/information to UEs constrained by weak received power resulting from LOS obstruction and/or path loss. The proposed MEH-R is designed to overcome two cardinal issues with existing RF energy harvesting systems, namely (i) small RF structural footprint; and (ii) low energy absorption efficiency due to low energy density. These issues jointly constitute the major factor that limits the energy output of existing harvesting systems. By taking advantage of its large structural size (1 m^2 or larger) and being deployed in an area of high RF power density, the MEH-R collects with high efficiency the energy of incident waves radiated by multiple ambient and dedicated RF energy sources such as the HAPs, BSs, energy stations (ESs), and space solar power satellites (SSPSs). Planar (intermediate) metasurfaces mounted on building facades also reflect RF energy/information signals toward the MEH-R, increasing the density of the impinging input RF power for conversion into substantial DC power [73]. In the following sequel, we elaborate on the three main constituents of the proposed system.

1) MEH-R

The conceptualized energy harvester-reflector shown in Fig. 23 is composed of five components: (i) large metasurface antenna of at least 1 m^2 dimension that can be reconfigured by a field programmable gate array (FPGA) encoder; (ii) corporate feed network; (iii) impedance matching network; (iv) rectifier circuit; and (v) charging zone. The large metasurface antenna size provides the desired aperture field distribution for high energy harvesting efficiency in densely deployed small cell networks. The corporate feed network combines the received RF power into a single outlet for rectification. The impedance matching network and the rectifier circuit perform the process of RF-DC conversion. Finally, the charging zone, which is an extension from the system's energy storage component, is where UEs can be charged in a plug-and-play manner.

2) MWPN

The envisioned wireless powered network operates in high microwave or mmWave band with a high concentration of

small cell networks. The small-cell HAPs are overlayed by a macro-cell BS, and both the HAPs and BS collectively provide a high-density ambient RF power for harvesting by the MEH-R. Besides, dedicated ESs and SSPS are present to increase the RF energy impinging on the MEH-R. Furthermore, the WPCN and SWIPT features are activated in the network, enabled by ESs and HAPs/BS, respectively. While WPCN allows UEs to exclusively harvest energy from the energy-only bearing RF fields transmitted by ESs, SWIPT offers UEs the opportunity to both harvest energy and extract information from the same received RF signals from the HAPs and BS. To optimize the network environment against path loss and LOS obstruction, planar metasurfaces are strategically deployed on building facades around the network as intermediaries to smartly control the RF wave propagation.

3) SSPS

The sun's unlimited constant energy supply is available in space, where solar energy harvesting is unaffected by weather conditions and day/night cycles. SSPS is an emerging paradigm, where satellites are deployed in space to generate DC power from sunlight using photovoltaics, which is then converted into microwave energy that can be beamed down to earth [74], e.g. to the MEH-R using WPT.

Compared to conventional rectennas, the proposed MEH-R has numerous potential advantages including: large aperture area that allows for high-capacity energy harvesting and energy reflection, low cost, ease of fabrication and assembly, and relatively insensitive to the angle of arrival and polarization of impinging RF signals. With such a configuration, we envisage that the energy harvested from the proposed system could reach such a level that it may complement the main grid to power a section of household DC appliances such as LED lighting, laptops, and other electronic gadgets by having them connected to the charging zone.

VI. CONCLUSION

The demand for anytime, anywhere, wireless recharging of communication devices through ambient and/or dedicated RF energy sources is continuously on the rise. This paper provided a comprehensive review of recent WPT and WPE approaches based on metasurface technology. We also surveyed their use in WPCN, SWIPT, and mmWave communication for not only enhancing the efficiency, but also facilitating the practical realization of WPT and WEH systems in future networks. In addition, we presented our futuristic metasurface-enabled RF energy harvesting and power transfer system, which could leverage the combined potentials of the discussed technologies to achieve optimal end-to-end energy delivery for the next generation of wireless networks.

REFERENCES

[1] A. Costanzo, M. Dionigi, D. Masotti, M. Mongiardo, G. Monti, L. Tarricone, and R. Sorrentino, "Electromagnetic energy harvesting and wireless power transmission: A unified approach," *Proc. IEEE*, vol. 102, no. 11, pp. 1692–1711, Nov. 2014.

[2] M. Alsharif, J. Kim, and J. Kim, "Green and sustainable cellular base stations: An overview and future research directions," *Energies*, vol. 10, no. 5, p. 587, Apr. 2017.

[3] M. H. Alsharif, A. H. Kelechi, M. A. Albreem, S. A. Chaudhry, M. S. Zia, and S. Kim, "Sixth generation (6G) wireless networks: Vision, research activities, challenges and potential solutions," *Symmetry*, vol. 12, no. 4, p. 676, Apr. 2020.

[4] Y. Kishiyama, D. Kitayama, S. Suyama, and Y. Hokazono, "Field experiments on millimeter-wave radio technology for 5G evolution," *NTT Docomo Tech. J.*, vol. 22, no. 3, pp. 33–43, 2021.

[5] L. Sanguinetti, E. Bjornson, and J. Hoydis, "Toward massive MIMO 2.0: Understanding spatial correlation, interference suppression, and pilot contamination," *IEEE Trans. Commun.*, vol. 68, no. 1, pp. 232–257, Jan. 2020.

[6] J. Guo, H. Zhang, and X. Zhu, "Theoretical analysis of RF-DC conversion efficiency for class-F rectifiers," *IEEE Trans. Microw. Theory Techn.*, vol. 62, no. 4, pp. 977–985, Apr. 2014.

[7] C. Liaskos, S. Nie, A. Tsioliaridou, A. Pitsillides, S. Ioannidis, and I. Akyildiz, "A new wireless communication paradigm through software-controlled metasurfaces," *IEEE Commun. Mag.*, vol. 56, no. 9, pp. 162–169, Sep. 2018.

[8] A. A. G. Amer, S. Z. Sapuan, N. Nasimuddin, A. Alphones, and N. B. Zinal, "A comprehensive review of metasurface structures suitable for RF energy harvesting," *IEEE Access*, vol. 8, pp. 76433–76452, 2020.

[9] L. Li, X. Zhang, C. Song, and Y. Huang, "Progress, challenges, and perspective on metasurfaces for ambient radio frequency energy harvesting," *Appl. Phys. Lett.*, vol. 116, no. 6, Feb. 2020, Art. no. 060501.

[10] A. A. Eteng, H. H. Goh, S. K. A. Rahim, and A. Alomainy, "A review of metasurfaces for microwave energy transmission and harvesting in wireless powered networks," *IEEE Access*, vol. 9, pp. 27518–27539, 2021.

[11] D. Shrekenhamer, W. Xu, S. Venkatesh, D. Schurig, S. Sonkusale, and W. J. Padilla, "Experimental realization of a metamaterial detector focal plane array," *Phys. Rev. Lett.*, vol. 109, no. 17, Oct. 2012, Art. no. 177401.

[12] Z. Zhang, H. Pang, A. Georgiadis, and C. Cecati, "Wireless power transfer—An overview," *IEEE Trans. Ind. Electron.*, vol. 66, no. 2, pp. 1044–1058, Feb. 2019.

[13] C. R. Valenta and G. D. Durgin, "Harvesting wireless power: Survey of energy-harvester conversion efficiency in far-field, wireless power transfer systems," *IEEE Microw. Mag.*, vol. 15, no. 4, pp. 108–120, Jun. 2014.

[14] L. Li, X. Zhang, C. Song, W. Zhang, T. Jia, and Y. Huang, "Compact dual-band, wide-angle, polarization- angle-independent rectifying metasurface for ambient energy harvesting and wireless power transfer," *IEEE Trans. Microw. Theory Techn.*, vol. 69, no. 3, pp. 1518–1528, Mar. 2021.

[15] L. G. de Carli, Y. Juppa, A. J. Cardoso, C. Galup-Montoro, and M. C. Schneider, "Maximizing the power conversion efficiency of ultra-low-voltage CMOS multi-stage rectifiers," *IEEE Trans. Circuits Syst. I, Reg. Papers*, vol. 62, no. 4, pp. 967–975, Apr. 2015.

[16] K. W. Choi, S. I. Hwang, A. A. Aziz, H. H. Jang, J. S. Kim, D. S. Kang, and D. I. Kim, "Simultaneous wireless information and power transfer (SWIPT) for Internet of Things: Novel receiver design and experimental validation," *IEEE Internet Things J.*, vol. 7, no. 4, pp. 2996–3012, Apr. 2020.

[17] R. Jiang, K. Xiong, P. Fan, Y. Zhang, and Z. Zhong, "Optimal design of SWIPT systems with multiple heterogeneous users under non-linear energy harvesting model," *IEEE Access*, vol. 5, pp. 11479–11489, 2017.

[18] M. Wagih, A. S. Weddell, and S. Beeby, "Millimeter-wave textile antenna for on-body RF energy harvesting in future 5G networks," in *Proc. IEEE Wireless Power Transf. Conf. (WPTC)*, Jun. 2019, pp. 245–248.

[19] Y. J. Yoo, Y. J. Kim, and Y. Lee, "Perfect absorbers for electromagnetic wave, based on metamaterials," *J. Korean Phys. Soc.*, vol. 67, no. 7, pp. 1095–1109, Oct. 2015.

[20] E. Unal, F. Dincer, E. Tetik, M. Karaaslan, M. Bakir, and C. Sabah, "Tunable perfect metamaterial absorber design using the golden ratio and energy harvesting and sensor applications," *J. Mater. Sci., Mater. Electron.*, vol. 26, no. 12, pp. 9735–9740, 2015.

[21] O. M. Ramahi, T. S. Almoneef, M. AlShareef, and M. S. Boybay, "Metamaterial particles for electromagnetic energy harvesting," *Appl. Phys. Lett.*, vol. 101, no. 17, Oct. 2012, Art. no. 173903.

[22] B. Alavikia, T. S. Almoneef, and O. M. Ramahi, "Complementary split ring resonator arrays for electromagnetic energy harvesting," *Appl. Phys. Lett.*, vol. 107, no. 3, Jul. 2015, Art. no. 033902.

[23] B. Alavikia, T. S. Almoneef, and O. M. Ramahi, "Wideband resonator arrays for electromagnetic energy harvesting and wireless power transfer," *Appl. Phys. Lett.*, vol. 107, no. 24, Dec. 2015, Art. no. 243902.

[24] A. Ghaneizadeh, K. Mafinezhad, and M. Joodaki, "Design and fabrication of a 2D-isotropic flexible ultra-thin metasurface for ambient electromagnetic energy harvesting," *AIP Adv.*, vol. 9, no. 2, Feb. 2019, Art. no. 025304.

[25] X. Zhang, H. Liu, and L. Li, "Electromagnetic power harvester using wide-angle and polarization-insensitive metasurfaces," *Appl. Sci.*, vol. 8, no. 4, p. 497, Mar. 2018.

[26] P. Xu, S.-Y. Wang, and W. Geyi, "Design of an effective energy receiving adapter for microwave wireless power transmission application," *AIP Adv.*, vol. 6, no. 10, Oct. 2016, Art. no. 105010.

[27] B. Ghaderi, V. Nayyeri, M. Soleimani, and O. M. Ramahi, "A novel symmetric ELC resonator for polarization-independent and highly efficient electromagnetic energy harvesting," in *IEEE MTT-S Int. Microw. Symp. Dig.*, Sep. 2017, pp. 1–3.

[28] B. Ghaderi, V. Nayyeri, M. Soleimani, and O. M. Ramahi, "Pixelated metasurface for dual-band and multi-polarization electromagnetic energy harvesting," *Sci. Rep.*, vol. 8, p. 13227, Sep. 2018.

[29] S. Costanzo and F. Venneri, "Polarization-insensitive fractal metamaterial surface for energy harvesting in IoT applications," *Electronics*, vol. 9, no. 6, p. 959, Jun. 2020.

[30] M. A. Aldhaeebi and T. S. Almoneef, "Planar dual polarized metasurface array for microwave energy harvesting," *Electronics*, vol. 9, no. 12, p. 1985, Nov. 2020.

[31] J.-F. Zürcher and F. E. Gardiol, *Broadband Patch Antennas*. London, U.K.: Artech House, 1995.

[32] S. Abeywickrama, R. Zhang, Q. Wu, and C. Yuen, "Intelligent reflecting surface: Practical phase shift model and beamforming optimization," *IEEE Trans. Commun.*, vol. 68, no. 9, pp. 5849–5863, Sep. 2020.

[33] M. El Badawe, T. S. Almoneef, and O. M. Ramahi, "A metasurface for conversion of electromagnetic radiation to DC," *AIP Adv.*, vol. 7, no. 3, Mar. 2017, Art. no. 035112.

[34] T. S. Almoneef, F. Erkmen, and O. M. Ramahi, "Harvesting the energy of multi-polarized electromagnetic waves," *Sci. Rep.*, vol. 7, no. 1, p. 14656, Dec. 2017.

[35] N. Supreeyatitikul, D. Torrungrueng, and C. Phongcharoenpanich, "Quadri-cluster broadband circularly-polarized sequentially-rotated metasurface-based antenna array for C-band satellite communications," *IEEE Access*, vol. 9, pp. 67015–67027, 2021.

[36] H. F. Huang and Z. P. Zhang, "A single fed wideband mode-reconfigurable OAM metasurface CP antenna array with simple feeding scheme," *Int. J. RF Microw. Comput.-Aided Eng.*, vol. 31, no. 13, pp. 1–8, 2020.

[37] F. Mirzavand, V. Nayyeri, M. Soleimani, and R. Mirzavand, "Efficiency improvement of WPT system using inexpensive auto-adaptive impedance matching," *Electron. Lett.*, vol. 52, no. 25, pp. 2055–2057, Dec. 2016.

[38] T. Zhang, W. Che, and H. Chen, "A wideband reconfigurable impedance matching network for complex loads," *IEEE Trans. Compon., Packag., Manuf. Technol.*, vol. 8, no. 6, pp. 1073–1081, Jun. 2018.

[39] E. Coskuner and J. J. Garcia-Garcia, "Metamaterial impedance matching network for ambient RF-energy harvesting operating at 2.4 GHz and 5 GHz," *Electronics*, vol. 10, no. 10, p. 1196, May 2021.

[40] M. Alibakhshikenari, B. S. Virdee, C. H. See, R. A. Abd-Alhameed, F. Falcone, and E. Limiti, "Impedance matching network based on metasurfaces (2-D Metamaterials) for electrically small antennas," in *Proc. IEEE Int. Symp. Antennas Propag. North Amer. Radio Sci. Meeting*, Jul. 2020, pp. 1953–1954.

[41] M. Alibakhshikenari, B. S. Virdee, A. A. Althuwayb, F. Falcone, and E. Limiti, "An innovative and simple impedance matching network using stacks of metasurface sheets to suppress the mismatch between antennas and RF front-end transceivers circuits," in *Proc. 15th Eur. Conf. Antennas Propag. (EuCAP)*, Mar. 2021, pp. 1–4.

[42] R. B. Greegor, C. G. Parazzoli, J. A. Nielsen, M. H. Tanielian, D. C. Vier, S. Schultz, and C. L. Holloway, "Demonstration of impedance matching using a mu-negative (MNG) metamaterial," *IEEE Antennas Wireless Propag. Lett.*, vol. 8, pp. 92–95, 2009.

[43] X. Duan, X. Chen, Y. Zhou, L. Zhou, and S. Hao, "Wideband metamaterial electromagnetic energy harvester with high capture efficiency and wide incident angle," *IEEE Antennas Wireless Propag. Lett.*, vol. 17, no. 9, pp. 1617–1621, Sep. 2018.

[44] L. KangHyeok and S. K. Hong, "Rectifying metasurface with high efficiency at low power for 2.45 GHz band," *IEEE Antennas Wireless Propag. Lett.*, vol. 19, no. 12, pp. 2216–2220, Dec. 2020.

[45] W. Lee, S.-I. Choi, H.-I. Kim, S. Hwang, S. Jeon, and Y.-K. Yoon, "Metamaterial-integrated high-gain rectenna for RF sensing and energy harvesting applications," *Sensors*, vol. 21, no. 19, p. 6580, Oct. 2021.

[46] X. Duan, X. Chen, and L. Zhou, "A metamaterial electromagnetic energy rectifying surface with high harvesting efficiency," *AIP Adv.*, vol. 6, no. 12, Dec. 2016, Art. no. 125020.

[47] G. T. Oumbé Tékam, V. Ginis, J. Danckaert, and P. Tassin, "Designing an efficient rectifying cut-wire metasurface for electromagnetic energy harvesting," *Appl. Phys. Lett.*, vol. 110, no. 8, Feb. 2017, Art. no. 083901.

[48] M. Song, A. Krasnok, R. Yafyasov, P. Belov, and P. Kapitanova, "Obstruction tolerant metasurface-based wireless power transfer system for multiple receivers," *Photon. Nanostruct.-Fundam. Appl.*, vol. 41, Sep. 2020, Art. no. 100835.

[49] M. Di Renzo, K. Ntontin, J. Song, F. H. Danufane, X. Qian, F. Lazarakis, J. D. Rosny, D.-T. Phan-Huy, O. Simeone, R. Zhang, S. Tretyakov, and S. Shamai, "Reconfigurable intelligent surfaces vs. relaying: Differences, similarities, and performance comparison," *IEEE Open J. Commun. Soc.*, vol. 1, pp. 798–807, 2020.

[50] T. S. Rappaport, Y. Xing, O. Kanhere, S. Ju, A. Madanayake, S. Mandal, A. Alkhateeb, and G. C. Trichopoulos, "Wireless communications and applications above 100 GHz: Opportunities and challenges for 6G and beyond," *IEEE Access*, vol. 7, pp. 78729–78757, 2019.

[51] H. J. Visser, S. Keyrouz, and A. B. Smolders, "Optimized rectenna design," *Wireless Power Transf.*, vol. 2, no. 1, pp. 44–50, Mar. 2015.

[52] W. Khawaja, O. Ozdemir, Y. Yapici, F. Erden, and I. Guvenc, "Coverage enhancement for NLOS mmWave links using passive reflectors," *IEEE Open J. Commun. Soc.*, vol. 1, pp. 263–281, 2020.

[53] X. Liu, Z. Wen, D. Liu, J. Zou, and S. Li, "Joint source and relay beamforming design in wireless multi-hop sensor networks with SWIPT," *Sensors*, vol. 19, no. 1, p. 182, Jan. 2019.

[54] X. Luo, M. Pu, X. Ma, and X. Li, "Taming the electromagnetic boundaries via metasurfaces: From theory and fabrication to functional devices," *Int. J. Antennas Propag.*, vol. 2015, Oct. 2015, Art. no. 204127.

[55] B. Lyu, P. Ramezani, D. T. Hoang, S. Gong, Z. Yang, and A. Jamalipour, "Optimized energy and information relaying in self-sustainable IRS-empowered WPCN," *IEEE Trans. Commun.*, vol. 69, no. 1, pp. 619–633, Jan. 2021.

[56] Y. Zheng, S. Bi, Y. J. Zhang, Z. Quan, and H. Wang, "Intelligent reflecting surface enhanced user cooperation in wireless powered communication networks," *IEEE Wireless Commun. Lett.*, vol. 9, no. 6, pp. 901–905, Jun. 2020.

[57] P. Zeng, Q. Wu, and D. Qiao, "Energy minimization for IRS-aided WPCNs with non-linear energy harvesting model," *IEEE Wireless Commun. Lett.*, vol. 10, no. 11, pp. 2592–2596, Nov. 2021.

[58] Y. Xu, Z. Gao, Z. Wang, C. Huang, Z. Yang, and C. Yuen, "RIS-enhanced WPCNs: Joint radio resource allocation and passive beamforming optimization," *IEEE Trans. Veh. Technol.*, vol. 70, no. 8, pp. 7980–7991, Aug. 2021.

[59] D. Niyato, D. I. Kim, M. Maso, and Z. Han, "Wireless powered communication networks: Research directions and technological approaches," *IEEE Wireless Commun.*, vol. 24, no. 6, pp. 88–97, Dec. 2017.

[60] Q. Wu and R. Zhang, "Weighted sum power maximization for intelligent reflecting surface aided SWIPT," *IEEE Wireless Commun. Lett.*, vol. 9, no. 5, pp. 586–590, May 2020.

[61] L. Zhao, Z. Wang, and X. Wang, "Wireless power transfer empowered by reconfigurable intelligent surfaces," *IEEE Syst. J.*, vol. 15, no. 2, pp. 2121–2124, Jun. 2021.

[62] C. Pan, H. Ren, K. Wang, M. Elkashlan, A. Nallanathan, J. Wang, and L. Hanzo, "Intelligent reflecting surface aided MIMO broadcasting for simultaneous wireless information and power transfer," *IEEE J. Sel. Areas Commun.*, vol. 38, no. 8, pp. 1719–1734, Aug. 2020.

[63] Q. Wu and R. Zhang, "Joint active and passive beamforming optimization for intelligent reflecting surface assisted SWIPT under QoS constraints," *IEEE J. Sel. Areas Commun.*, vol. 38, no. 8, pp. 1735–1748, Aug. 2020.

[64] N. Shlezinger, O. Dicker, Y. C. Eldar, I. Yoo, M. F. Imani, and D. R. Smith, "Dynamic metasurface antennas for uplink massive MIMO systems," *IEEE Trans. Commun.*, vol. 67, no. 10, pp. 6829–6843, Oct. 2019.

[65] H. Luan, C. Chen, W. Chen, L. Zhou, H. Zhang, and Z. Zhang, "Mutual coupling reduction of closely E/H-plane coupled antennas through metasurfaces," *IEEE Antennas Wireless Propag. Lett.*, vol. 18, no. 10, pp. 1996–2000, Oct. 2019.

[66] W. Meng, X. He, Y. Li, H. Wu, and C. Yin, "Wireless power transfer via intelligent reflecting surface-assisted millimeter wave power beacons," in *Proc. IEEE 93rd Veh. Technol. Conf. (VTC-Spring)*, Apr. 2021, pp. 1–6.

[67] F. Xiao, W. Yang, W. Che, Q. Xue, and W. Zhang, "High-efficiency millimeter-wave wide-angle scanning phased array using metasurface," in *IEEE MTT-S Int. Microw. Symp. Dig.*, May 2021, pp. 1–3.

[68] J.-B. Gros, V. Popov, M. A. Odit, V. Lenets, and G. Lerosey, "A reconfigurable intelligent surface at mmWave based on a binary phase tunable metasurface," *IEEE Open J. Commun. Soc.*, vol. 2, pp. 1055–1064, 2021.
[69] C.-C. Chung, F.-P. Lai, S.-X. Huang, and Y.-S. Chen, "Anisotropic metasurface with asymmetric propagation of electromagnetic waves and enhancements of antenna gain," *IEEE Access*, vol. 9, pp. 90295–90305, 2021.
[70] S. M. Patole, M. Torlak, D. Wang, and M. Ali, "Automotive radars: A review of signal processing techniques," *IEEE Signal Process. Mag.*, vol. 34, no. 2, pp. 22–35, Mar. 2017.
[71] A. E. Olk, P. E. M. Macchi, and D. A. Powell, "High-efficiency refracting millimeter-wave metasurfaces," *IEEE Trans. Antennas Propag.*, vol. 68, no. 7, pp. 5453–5462, Jul. 2020.
[72] M. Holmberg, D. Dancila, A. Rydberg, B. Hjrvarsson, U. Jansson, J. J. Marattukalam, N. Johansson, and J. Andresson, "On surface losses in direct metal laser sintering printed millimeter and submillimeter waveguides," *J. Infr., Millim., Terahertz Waves*, vol. 39, no. 6, pp. 535–545, Jun. 2018.
[73] J. Hu, K. Yang, G. Wen, and L. Hanzo, "Integrated data and energy communication network: A comprehensive survey," *IEEE Commun. Surveys Tuts.*, vol. 20, no. 4, pp. 3169–3219, 4th Quart., 2018.
[74] N. Shinohara and S. Kawasaki, "Recent wireless power transmission technologies in Japan for space solar power station/satellite," in *Proc. IEEE Radio Wireless Symp.*, Jan. 2009, pp. 13–15.

HENRY OJUKWU received the B.Sc. degree in computer science and the M.Eng. degree in telecommunications engineering from the University of Malaya, Malaysia, in 2013 and 2015, respectively. He is currently pursuing the Ph.D. degree with the Department of Electrical and Electronic Engineering, Auckland University of Technology, New Zealand. His research interests include RF frequency energy harvesting, wireless powered communications, metamaterials, metasurfaces, RF design, antennas, and propagation.

BOON-CHONG SEET (Senior Member, IEEE) received the Ph.D. degree from Nanyang Technological University, Singapore, in 2005. He was a Research Fellow with the National University of Singapore, under the Singapore—Massachusetts Institute of Technology Alliance Program. Since 2007, he has been with the Department of Electrical & Electronic Engineering, Auckland University of Technology, New Zealand, where he is currently an Associate Professor and the Head of Department. He is also the Founding Leader of the Wireless InnovationS in Engineering (WISE) Research Group. His research interests include the fields of info-communication technologies (ICT), with a focus on emerging communication, computing, and sensing technologies for smart systems.

SAEED UR REHMAN (Senior Member, IEEE) received the M.E. and Ph.D. degrees in electrical and electronic engineering from the University of Auckland, New Zealand, in 2009 and 2015, respectively. He is currently a Senior Lecturer with the College of Science and Engineering, Flinders University, Adelaide, Australia. Prior to joining Flinders University, he has worked as a Lecturer with the Auckland University of Technology, from 2017 to 2019, and a Senior Lecturer/ an Academic Leader with the Unitec Institute of Technology, Auckland, New Zealand, from 2014 to 2017. His current research interests include physical-layer security (in wireless devices and embedded systems), privacy-aware embedded systems in health care, and visible light communication.